Low Power Microrobotics
Utilizing Biologically Inspired Energy Generation

October 1, 2011 through September 31, 2012

Principal Investigator: Gregory P. Scott, Ph.D.
Co-Investigator: Leonard Tender, Ph.D.
Co-Investigator: Stephen Arnold, D.Sc.

This page intentionally left blank.

Abstract

The Low Power Microrobotics (LPM) project is a NASA NIAC-funded multi-disciplinary research effort involving the research and advancement of low power electronics, low power mobility and their integration with state of the art microbial fuel cell for power generation. The goal of this project was to advance the capabilities of each of these systems with a 10-year future target of a near one kilogram space exploration vehicle that contains each of these systems. In order to accomplish this task, each system was investigated independently in order to establish the power requirements/limitations while considering how each system affects the other systems. This was performed through numerous trade studies and experimental work, primarily focused around the power capacity of the microbial fuel cell base-lined for this project and how its strengths and limitations affected the design of the remaining onboard systems. Finally an end-to-end system test utilized a microbial fuel cell to charge a super capacitor through an energy harvesting circuit, which was discharged to activate a robotic locomotion system.

Table of Contents

Executive Summary

Background

In the past decade, more than $10M has been invested in the development of "waste-to-energy" research at the NRL and the focus of harnessing the energy from microbial sources. In addition, nearly $30M in research funding has been awarded to space robotics research, including the development of space qualified actuators, mechanisms and electronics. Considering the extensive research experience in these areas, a team was assembled at the NRL to investigate low power microrobotic systems powered by microbial fuel cells.

The Primary Investigator for this program (Dr. Gregory P. Scott) was awarded the NRL's Karles' Fellowship in 2010 totaling nearly $250k towards the investigation of novel space robotics research including low power microrobotics, manipulator development, and robotic control systems. Utilizing a portion of this funding, he began investigating and developing initial proposals for small robotic systems technology maturity. One of the most significant areas where research advancement is required in the field of microrobotic systems is with regards to power generation and distribution. Looking into alternative and far-out technology options for remedying this problem, he began to investigate the consideration of microbial fuel cells as the primary power generation system for a robotic system along with program co-investigator Dr. Leonard Tender, a subject matter expert in waste-to-energy research.

One significant problem with using a microbial fuel cell for power generation is the exceptionally low constant power availability of these systems, especially at the lower masses and volumes required by microrobotic systems (in the very low milliwatts). Therefore, a paradigm shift in the approach to onboard microelectronics would also be required to utilize this technology. Further discussion with Dr. Stephen Arnold, subject matter expert in spacecraft electronics, led to the consideration of a multi-tiered approach to powering the onboard electronics, while also actively working to reduce the electrical requirements of the onboard components themselves.

From this initial investigation and utilizing the expertise of this team and others, a research project was awarded by the NASA NIAC program office to investigate low power microrobotic systems utilizing biologically inspired energy generation.

Accomplishments and Significance

The team conducted many experiments and accomplished several goals during the execution of this project. These accomplishments were made in three distinct research areas:

- Low power mobility systems for robot locomotion on planetary surfaces;
- electronics with low power requirements for core robot control functionality;
- biologically-inspired power generation techniques for long duration vehicle lifetime.

Through the work performed on this study, the technology readiness level of each system was advanced, allowing for an increased understanding of how these systems operated independently, as well as how they could interact together. Experiments showed that the self-contained pure-culture microbial fuel cell produced an effective amount of power (2.4 mW at 0.3 V) that could be harnessed by an energy harvesting circuit. Low power electronics were tuned to charge a super capacitor and eventually discharge the stored energy to activate an electromechanical

system. Two distinct low power mobility actuators were designed for operation in different environmental conditions.

In the final experiment, a benthic mesocosm sediment tank in the littoral high bay of the Laboratory for Autonomous Systems Research (LASR) was used as the microbial fuel cell power source. With an electrical output of 9 mA at 0.35 V, this fuel cell charged a 280 mF 3.6 V super capacitor through the energy harvesting circuit in less than 2 hours. The charged super capacitor was then discharged to operate the 3 V motor in a small walking robot for 13 seconds. This demonstrated the effective usage of a microbial fuel cell to locomote a robotic system utilizing low power electronics and an effective power management system.

The significance of the LPM project accomplishments translate to the following specific successes:

1. Further advancement and application of a dual-chamber pure culture microbial fuel cell;
2. Development of electrical storage and distribution subsystem at low power;
3. Design of efficient mechanisms to be powered from a biological source;
4. Proving the proposed concept through an end-to-end test of the microbial fuel cell to power an electromechanical output system.

Future Applications

The applications that exist from technology advanced through this research project are many. Microbial fuel cells have potential application in numerous industries as a power source. On larger scales, MFCs can support raw sewage treatment facilities as a catalyst for breaking down biological material and providing a power source in the process. On the small to medium scale, they could provide power to remote areas of the world, supplied only by the local environment. On the smaller power scale (but larger volumetric scale), a MFC has already been used to power a sensor systems deployed on a buoy to monitor the environmental conditions of a river.

Lowering the power requirements for electronics would revolutionize many industries. In the space industry, one of the most significant limiting issues on a spacecraft is the available power. Improving efficiencies or optimizing low power electronics would increase the lifetime of a spacecraft or reduce the overall power subsystem mass/volume requirements, allowing for reductions in mission costs. Applications of low power electronics in the mobile computing industry would help to increase battery life for mobile electronics, while the power harvesting capability would allow battery charging capability from non-traditional low power sources.

The design of low power electromechanical systems has driven the team to look more closely at the essential hardware required for actuation. Reduction of gearing requirements while selecting a comparable low voltage motor was a focus in one study, while consideration of a new locomotion approach through linear actuators was developed in another. The applications for more tuned electromechanical systems and a paradigm shift towards non-traditional motors have application in the space industry and beyond.

With further advances in each technology (such as improving the efficiency of the cathode reaction of the low volume microbial fuel cell or improving electromechanical efficiency for locomotion systems targeted to low gravity environments), a future application of these interdisciplinary areas could include a low power microrobotic system for low gravity environments using a microbial fuel cell to generate electricity.

Introduction

The Naval Research Laboratory (NRL) is a leading research organization in each of the technology focus areas that are presented in this report. In the past decade, more than $10M has been invested in the development of "waste-to-energy" research and the focus of harnessing the energy from microbial sources. Nearly $30M in research funding has been awarded to space robotics research, including the development of space qualified actuators, mechanisms and electronics. Fusing these technology research areas together, a team was formed to investigate low power microrobotic systems powered by microbial fuel cells.

The Primary Investigator for this program (Dr. Gregory P. Scott) was awarded the NRL's Karles' Fellowship in 2010 totaling nearly $250k towards the investigation of novel space robotics research including low power microrobotics, manipulator development, and robotic control systems. Utilizing a portion of this funding, he began investigating and developing initial proposals for small robotic systems technology maturity. One of the most significant areas where research advancement is required in the field of microrobotic systems is with regards to power generation and distribution. Looking into alternative and future technology options for remedying this problem, he began to investigate the consideration of microbial fuel cells as the primary power generation system for a robotic system along with program co-investigator Dr. Leonard Tender, a subject matter expert in waste-to-energy research.

One significant problem with using a microbial fuel cell for power generation is the exceptionally low constant power availability of these systems, especially at the lower masses and volumes required by microrobotic systems (in the very low milliwatts). Therefore, a paradigm shift in the approach to onboard microelectronics would also be required to utilize this technology. Further discussion with Dr. Stephen Arnold, subject matter expert in spacecraft electronics, led to a consideration of a multi-tiered approach to powering the onboard electronics, while also actively working to reduce the electrical requirements of the onboard components themselves.

From this initial investigation and utilizing the expertise of this team and others, a research project was proposed and funded by the NASA NIAC program office to investigate low power microrobotic systems utilizing biologically inspired energy generation.

Research Proposal

The primary objective proposed for this research project was to advance the state of the art of an integrated robotic system united from three different research areas (low power electronics, low power mobility, microbial fuel cell energy generation). The expected research outcomes would advance the state of the art of this integrated system from the TRL 1 concept phase to each of these components working both independently and jointly on a test bench. The target vehicle onto which these technologies would be directed is a near one-kilogram robot. The resulting outcome of this work would include an off-board MFC that will provide power to the off-board electronics boards, which would control the vehicle locomotion system.

The proposal was made that, upon completion of this research, the following advances would be made:

- an off-board low power electronics controller board will be built and power consumption of all components monitored and controlled;
- a novel low power robotic locomotion system would be designed for surface or microgravity mobility on a one-kilogram sized vehicle;
- an off-board microbial fuel cell will be tested to determine power output and used to charge the required energy storage device.

Project Plan

In order to achieve these objectives, a 1 year project plan was developed to follow three independent research streams, culminating in an integrated test of the developed hardware.

The first stream follows the development of the low power robotic locomotion system. Due to the high power requirements of motors in traditional wheeled/tracked locomotion, non-traditional methodologies will need to be considered to reduce (or eliminate) onboard electromechanical hardware for locomotion. Slow-charging spring-loaded hopping locomotion is considered for ground mobility and preliminary research has already been undertaken in this direction. Other ground-based locomotion methodologies (such as a single motor driving a simple tripod gait statically stable locomotion system or compressed air propulsion) will also be considered in more detail during the initial phases of research for this project.

The second stream follows the investigation into microbial fuel cells (MFCs). In the area of power generation, microbial fuel cells have been studied for a number of years. However, the infrastructure required to effectively grow microbe colonies and generate electricity currently includes large pumps, high power requirements and significant system control. This research stream will focus on a pure culture anaerobic bacteria, such as *Geobacter sulfurreducens*, as the core of the microbial fuel cell-based power system. This low power generation technology would have an exceptionally long lifetime, beneficial for recharging onboard batteries or capacitors for long duration scouting missions. Utilizing these microbes, a full-scale MFC will be used to determine the power available to the system. Further research will then be conducted to propose methodologies to reduce the currently required infrastructure in order to reach a mass/volume that is consistent with the vehicle mass/volume constraints.

The third stream follows the development of low power electronics for vehicle control. A power budget will be developed based on inputs from the MFC and proposed onboard power storage options (small super capacitors or battery cells), along with the output requirements of the locomotion system and additional onboard sensor systems that would be required for the mission. Research into low power electronics will be conducted to determine if power-intensive control electronics (such as microcontrollers or FPGAs) would be required or if older but less power-intensive systems (such as discrete logic components or flash-based schedule controllers) would be more appropriate. A prototype board will be built and the power consumption will be tested while operating the locomotion system designed for the vehicle.

Proposed Milestones

Through following these research streams, several significant results are expected to be achieved, while opening the door to new questions that could be addressed with further research. The following milestones were proposed for this study:

1. initial study into various low energy mobility systems and a proof-of-concept to be built from the most appropriate option,
2. selection of required baseline electro-mechanical hardware (if any) for locomotion with an effort to minimize power requirements,
3. off-board power management electronics to be designed and prototyped to control charging of onboard capacitors/cells from the MFCs
4. on-board scheduling management to provide power to locomotion system and associated hardware when needed,
5. consider existing MFC infrastructure to study the energy profile of the microbes to select the most appropriate microbe for this application,
6. utilize an off-board closed-loop pure culture MFC to provide power to the electronics and controller hardware,
7. propose methodology for minimizing MFC hardware infrastructure while maintaining acceptable power output levels,
8. propose a sensor suite to support the system, with consideration of sonar/camera, chemical/biological detection, data transmission, and other low power sensory capabilities,
9. test the proof-of-concept locomotion system with off-board electronics and off-board MFC to examine the system potential.

Related Research

Research has been completed on various projects relating to each area of this proposal. Each group has years of expertise in their respective fields and each was able to apply that expertise to the proposed project.

The Naval Center for Spacecraft Technology at the NRL has a proven track record of successfully producing strong results for internal and external research projects. The robotics group in the Control Systems Branch has participated in over $30M worth of spacecraft engineering and robotics research programs in the last decade. Key examples of this robotics research include:

- SUMO/FREND robotic arm – DARPA-sponsored technology development program aimed at designing and building a robotic payload capable of grappling and repositioning existing space assets [1].
- LIIVe – a DARPA-sponsored subsystem upgrade to provide low power onboard computer vision, wireless network communication and various capabilities to the LIIVe robotic free-flyer that will travel to the International Space Station [2].
- RAFT – a DARPA-sponsored seedling project to develop a prototype biologically inspired robotic arm to autonomously refuel unmanned Navy vessels [3].
- QbX – Integration of experimental satellite communications payload into a small CubeSat form factor, requiring significant reduction in electronics size, weight and power [4].

The microbial fuel cell group in the Center for Bio/Molecular Science and Engineering at the NRL has a proven track record of developing novel biological power generation systems both within the laboratory and in the field. They have provided real-world demonstration of these systems as a practical alternative to batteries for low power consuming applications. They have had much recent success with the proof-of-concept practical applications of MFC-powered maritime sensors being deployed into the field. However, MFCs have yet to be used to power unmanned vehicles through research at the NRL, which is covered in this research program. Key examples of ongoing MFC research include:

- Benthic microbial fuel cells (BMFCs) – a type of MFC that utilizes organic matter residing in marine sediment as the fuel and oxygen residing in overlying water as the oxidant, to persistently power oceanographic sensors. Currently at TRL 5, the BMFC has undergone multiple rounds of optimization and demonstrations [5].
- Pure culture MFCs – a variant of *Geobacter sulfurreducens* grown on an electrode and recovered for testing was found to have an enhanced power and current density more than 5x greater than the naturally occurring microorganism [6].
- Gates Foundation – investigating the development of microbial fuel cells to generate electricity from wastewater in developing countries.
- DC Water Authority – currently working with the local water authority to determine the feasibility of using microbial fuel cells offset power consumption of their treatment process.

Through this expertise in each research field, the team was strongly positioned to take on the challenges required by this NASA NIAC Phase I research project.

Project Resources

Personnel

Team Qualifications
The Naval Research Laboratory has an extensive history in related robotics and microbial fuel cell research that led to the development of this research project. This includes space qualified robotics research and applied spacecraft technology development (including over 100 satellite launches since the NRL's creation). The NRL is also a world leader in the area of waste-to-energy research with basic and applied research projects advancing this technology through many avenues. Together, these groups will focus on a long-term directed research stream to apply this novel power generation approach towards a space qualified robotic explorer.

Principal Investigator – Dr. Gregory P. Scott
Dr. Scott earned his Ph.D. in the field of space robotics with a focus on biologically inspired legged vehicles and their mobility over complex terrain. He joined the NRL under the Karles' Fellowship Program in 2010 and is developing a research portfolio to include biologically inspired robotics, vehicle mobility in complex terrain, space robotics and other related areas. Prior to working with the NRL, he completed his Ph.D. research at the Surrey Space Center at the University of Surrey in Guildford, England in 2009. He also earned his M.Sc. in Space

Architecture from the University of Houston and a B.Sc. in Aerospace Engineering from the Pennsylvania State University. Dr. Scott was selected as a NASA NIAC Fellow and awarded Phase I funding for this low power microrobotics project. For this project, Dr. Scott was responsible for overseeing the locomotion system focus area, including the biologically inspired actuators, as well as overall system development requirements and project management.

Co-Investigator – Dr. Stephen P. Arnold
Dr. Arnold is a computer scientist/engineer in the Flight Systems section of the Naval Center for Space Technology (NCST) at the NRL in Washington, D.C. Dr. Arnold received his B.Sc. in Physics in 1997 from the University of Michigan, his M.Sc. in Computer Engineering from The George Washington University (GWU) in 2002, and his D.Sc. in Computer Engineering from GWU in 2010. He has been with NRL since 1997. The research within his Branch includes radiation effects in spacecraft electronics, advanced detectors ranging from the UV to the SWIR, MWIR, LWIR, and VLWIR, photovoltaics for space applications, and space technology demonstration experiments. He is a two time winner of the NRL Alan Berman Research Publication Award. He is a long-standing member of the IEEE. For the NIAC Phase I project, Dr. Arnold was responsible for the electronics focus area including the energy harvesting electronics development and the energy storage capabilities of the power subsystem.

Co-Investigator – Dr. Leonard M. Tender
Dr. Tender, a Branch Head and research chemist in the Center for Bio/Molecular Science and Engineering at the NRL, is the Department of Defense's leading science and technology expert in the field of bioelectrochemical systems, processes in which microorganisms are used to catalyze electrode reactions. Such processes include anode oxidation of organic matter for alternative power generation and wastewater treatment, and cathode reduction of carbon dioxide into liquid fuels. He earned his B.Sc. in Chemistry at MIT, and a Ph.D. in Chemistry at the UNC, Chapel Hill. For the NIAC Phase I project, Dr. Tender was responsible for the microbial fuel cell power generation focus area, including advancements to the fuel cell hardware and supported the energy harvesting process.

Additional Contributing Personnel
Mr. Clark Person received a M.Sc. in Electrical Engineering from Virginia Tech in 2008 and a B.Sc. in Electrical Engineering from Washington University in St. Louis in 2001. While studying at the Center for Power Electronics Systems at Virginia Tech, his research focused on multi-element resonant converters and soft-switching techniques in DC/DC converters. Other research interests include GaN power devices and spacecraft charging. He currently works as a power system design engineer in the Spacecraft Engineering Department at the Naval Research Laboratory.

Ms. Kyla Gregoire is a Ph.D. Candidate in the Department of Civil & Environmental Engineering at the University of Maryland. Her research focuses on energy-positive wastewater treatment, including integrated anaerobic digestion-microbial fuel cells (AD-MFCs). She has six years' experience with design of water & sanitation initiatives in Tanzania, Peru, and Haiti, most recently including the design of low cost AD system for the Partners in Health medical complex in Cange, Haiti. She is mentored by Dr. Leonard Tender at the Naval Research Laboratory and Dr. Stephanie Lansing in the Department of Environmental Science & Technology at the University of Maryland.

Brian Guenther is an undergraduate student at Rochester Institute of Technology working towards a B.Sc. in Mechanical Engineering. He is a member of the Formula SAE Racing Team, working with a team of student engineers to completely design, build, and test a prototype racecar for international competition. He expects to graduate in May 2013 and enter the workforce as a design engineer in the aerospace industry.

Mr. Frederick Bernard Harris, Jr. is currently working towards his a B.Sc. in Mechanical Engineering and has been awarded an academic scholarship each semester during his enrollment at Howard University. He completed a summer internship at the Naval Research Laboratory in Washington DC in 2012 under the HBCU/MI Summer Internship Program. While working there, Frederick focused primarily on the NASA NIAC Phase I project through motor sizing analysis and electrical energy analysis for a low power microrobotic locomotion system. His work was selected as the best project of the summer internship program, awarding him an academic stipend.

Equipment and Facilities
All facilities that were utilized for this research project are housed at the Naval Research Laboratory in Washington DC. There were several different laboratories throughout the NRL that were used for each aspect of the project.

Electrical Power System (EPS) Development Lab
Electronics testing and development was conducted in the Electrical Power System (EPS) Development Lab. General purpose instrumentation used in testing included oscilloscopes, multimeters, and data acquisition units. For testing purposes, the fuel cell input to the electronics was simulated using a general purpose lab power supply and a variety of different electrical components, which were pulled from EPS Development Lab stock. Electronics fabrication tools, such as solder irons, wire-wrap set, and assorted hand tools were also used to fabricate, wire, and modify hardware. Figure 1 shows the primary workspace used during this project in the EPS Development Lab.
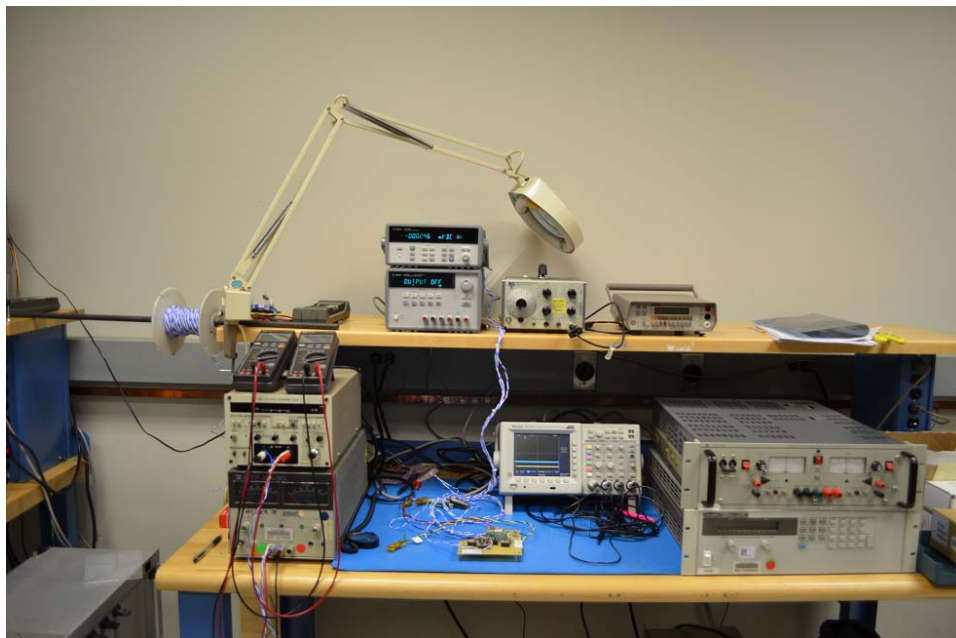
Figure 1 – Electrical Power System (EPS) Development Lab workspace (Credit: C. Person/NRL)

Laboratory for Microbial Electrochemistry

The Laboratory for Microbial Electrochemistry is headed by Dr. Leonard Tender in the Center for Biomolecular Science & Engineering at the US Naval Research Laboratory, and includes four permanent researchers. The breadth of the lab's work spans a number of areas related to bioelectrochemical systems including: (1) elucidating the mechanism of microbially-mediated electron transfer at electrode surfaces; (2) scale-up and deployment of benthic microbial fuel cells (BMFCs) for powering low power devices (e.g. sensors, monitoring devices) remotely deployed in marine environments drawing off organic matter in sediments and oxygen in overlying water and; (3) microbial fuel cells (MFCs) for energy-positive wastewater treatment in developing nations, DoD facilities, and US domestic wastewater treatment plants. Figure 2 shows one of the workspaces in the Laboratory for Microbial Electrochemistry used during this research.

Figure 2 – This experimental instrumentation in the Laboratory for Microbial Electrochemistry one of five 8-channel potentiostats that can be used to simultaneously investigate performance of multiple bioelectrochemical systems. (Credit: J. Harman/NRL)

Laboratory for Autonomous Systems Research (LASR) Littoral Lab

The Laboratory for Autonomous Systems Research (LASR) facility (shown in Figure 3) is a brand new world class research facility dedicated to bringing together scientists and engineers from diverse backgrounds to tackle common challenges in autonomy research at the intersection of their respective fields. LASR integrates science and technology components into research prototype systems and will become the nerve center for basic research that supports autonomous systems research for the Navy and Marine Corps.

Figure 3 – The Laboratory for Autonomous Systems Research (LASR) (Credit: J. Hartman/NRL)

Within the LASR, there are five primary environmental high bays, and the littoral high bay was utilized for this project. The littoral high bay includes various tanks and pools to support the evaluation of autonomous systems and power and energy systems in water environments. The

high bay is 54' by 76' by 28' tall overall and includes a 25' by 45' pool that is 5.5 feet deep. A 16-channel wave generator can provide directional waves within the tank while the opposite end can have a slope installed for autonomous vehicle access. The pool may be equipped with sand, mud, and stone to emulate various shorelines. The wave generator and slope can be removed to provide a larger constant depth space. Of particular interest to this project are the multiple benthic mesocosms for evaluation of sea-bottom energy harvesting using benthic microbial fuel cells (BMFCs). One of these mesocosms is shown in Figure 4.

Figure 4 – One benthic mesocosm in the littoral high bay of LASR with Dr. Tender (back to the camera) addressing Dr. John Holdren, Director of Science and Technology Policy and President Obama's Senior Science Advisor, along with other distinguished guests. (Credit: J. Hartman/NRL)

Utilizing the years of expertise from the personnel at the NRL and the world class facilities available on-site, the team was able to accomplish the tasks set forth in the project proposal. The next section of this report details the results obtained from each aspect of the research program.

Phase I Results

In Phase I, the team was able to advance the state of the art in low power microrobotics design and development. The core competencies in this research stem from three primary areas:

- Biologically inspired energy generation techniques for long duration vehicle lifetime;
- Electronics with low power requirements for core robot control, task scheduling, task execution, etc.;
- Low power mobility for robot locomotion either on planetary surfaces or free-floating.

Together, each of these areas of research promote the concept of microrobotic locomotion with a biologically-focused energy source and a low power approach to onboard electronics and control. The advancements in each individual research areas are summarized in the following

sections, with an emphasis on the final section detailing the expected results of the integration of each of these technological advancements prior to the completion of the Phase I research.

Microbial-based Energy Generation

Microbial fuel cells (MFCs) possess anode reactions that are catalyzed (accelerated) by microorganisms to generate electrical power at a range from less than 1 watt to more than 1 megawatt, theoretically. They promise relatively high energy density compared to lithium batteries and hydrogen fuel cells by utilizing biomass-derived fuels such as glucose and acetate which lack risk of explosion. Current results however suggest that MFCs may only achieve low power densities that support investigation for low power, long duration applications for which they may prove superior to existing power supplies based on energy density and safety. MFCs are also being investigated to generate electrical power from the biomass content of wastewater in order to offset energy consumption of wastewater treatment processes.

A MFC is a fuel cell in which the anode reaction is catalyzed (accelerated) by microorganisms. That is, the microorganisms oxidize the fuel and transfer the acquired electrons to the anode much faster than the anode can oxidize fuel itself. This enables generation of electrical power from biomass derived fuels that are naturally oxidized by microorganisms, such as glucose, acetate, and wastewater, for which conventional anode catalysts do not exist. Such fuels are renewable, relatively high in energy density, and non-explosive. While there are numerous types of microorganisms that can oxidize biomass derived fuels, only a very select group can transfer electrons directly to anodes. It was the discovery of this ability in 2002 [7] that accelerated interest in microbial fuel cells.

The most common type of MFC, diagrammed in Figure 5a, is comprised of two compartments (half-cells). An aqueous solution (anolyte) containing the microbial fuel is circulated through the anodic half-cell which houses the anode. An aqueous solution (catholyte) containing an oxidant, typically oxygen, is circulated through the cathodic half-cell which houses the cathode.
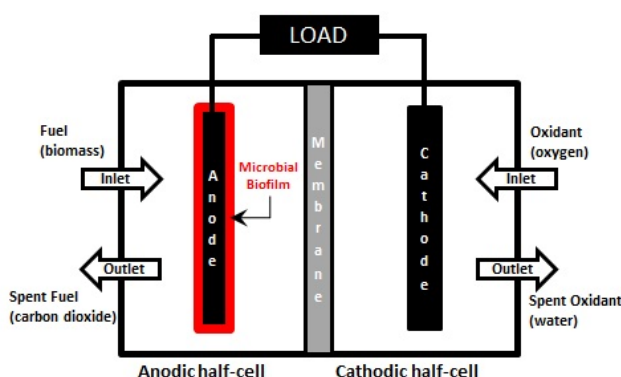

Figure 5 – a) A diagram of a microbial fuel cell.

Specific microorganisms will affix themselves to the anode surface forming a persistent film (biofilm) that catalyzes anode oxidation of the fuel. In return, the microorganisms derive benefit from the catalytic process, extracting a small portion of the potential energy of electrons passing through them from the fuel to the anode to satisfy their own energy. In this way, the microbial biofilm maintains itself and its catalytic activity does not wane as does the catalytic activity of conventional electrode catalysts. The electrons acquired by the anode from oxidation of fuel are

conducted through an external circuit to the cathode where they are consumed by reduction of oxidant. As in the case of conventional fuel cells, MFCs require a membrane to isolate the anode from the oxidant, while charge compensating ions to flow from the anode to the cathode. Inefficiencies in membrane material technologies is one particular area for future research, however this was not studied under the NIAC Phase I project.

Background Theory

The flow of electrons through the external circuit (noted as the load in Figure 5a) before re-bonding with the ions at the cathode constitutes an electrical current. Because the net reaction (oxidation of fuel and reduction of oxidant) is thermodynamically favorable (releases energy), the electrical current can occur spontaneously resulting in electrical power that can be utilized by an electrical power consuming device connected in series with the external circuit. A key obstacle to application of MFCs which will need to be addressed is the poor kinetic activity of oxygen reduction cathodes at neutral pH inherent to MFCs (unlike the high or low pH of hydrogen/oxygen fuel cells for which they were developed), greatly diminishing MFC power output.

A common MFC utilizes acetate as the fuel, either added to water or as found in wastewater, and oxygen as the oxidant. The net MFC reaction is described by the following chemical equation:

$$CH_3COOH + 2O_2 \rightarrow 2CO_2 + 2H_2O, DG0 = - 875 \text{ kJ/mole of acetate reacted}$$

which is the result of two coupled half reactions, the oxidation of acetate occurring at the anode:

$$CH_3COOH + 2H_2O \rightarrow 2CO_2 + 8H^+ + 8e^-$$
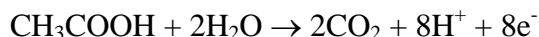
and the reduction of oxygen occurring at the cathode:

$$2O_2 + 8H^+ + 8e^- \rightarrow 4H_2O$$
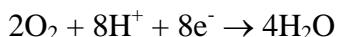
where oxidation of each mole of acetate (CH_3COOH) requires 2 moles of oxygen (O_2), forming 2 moles of carbon dioxide (CO_2) and 2 moles of water (H_2O), generating 875 kJ (243 Wh) of energy per mole of acetate consumed when performed with 100% efficiency. This equates to a theoretical upper limit of energy density of an acetate and oxygen consuming MFC of 14,600 kJ/kg (4050 Wh/kg) or 13,500 kJ/L (3750 Wh/L) assuming oxygen consumed is from the environment and that the mass and volume of the MFC is negligible compared to that of the fuel stock. By comparison, state of art lithium batteries can provide 1,300 kJ/kg (360 Wh/kg) or 975 kJ/L (270 Wh/L), hence the promise of very high energy density of MFCs when fully developed. Owing to the finite rate of microbial catalyzed anode oxidation of biomass (on order of 10^{-3} A/cm^2 vs. on order of 1 A/cm^2 for platinum catalyzed anode oxidation of hydrogen), and poor kinetics of oxygen reduction at neutral pH and low ion permeability of conventional ion exchange membranes at low pH and in complex ionic media inherent to MFCs, typical MFC power density (on the order of 0.005 W/L) is orders of magnitude lower than theoretically possible if these limitation can be addressed. Dr. Tender is currently leading a research effort funded by the Office of Naval Research (ONR) to specifically to address these limitations and which will directly benefit the future direction of this research [8].

MFC Performance Evaluation

The MFC used in the Phase I study (shown in Figure 5b) was developed as part of a Gates Foundation funded project to investigate the use of MFCs to generate useful electrical power from the organic matter content of waste water.

Dual-chamber MFC reactors were fabricated out of plexiglass and graphite block, and were designed to mimic the large-scale baffled anaerobic reactors that achieve maximum treatment efficiency in wastewater unit processes. Both the anode and the cathode internal volumes are 100 mL each, while the overall fuel cell dimensions are 21.5 cm x 21.5 cm x 3.9 cm (1800 mL total volume). Plug flow conditions were achieved with a 10:1:1.5 (length:width:depth) ratio, allowing the fuel to flow through the chambers and maximize the contact with the membrane. The dual-chamber allowed for the use of a pseudo membrane electrode assembly (MEA) in which the electrodes were mechanically compressed to the membrane to minimize electrode spacing and maximize power production. The MEA utilized untreated carbon cloth as both the anode and cathode material (YS-A Series Nippon fabrics, Japan) which was mechanically pressed against either side of an anion exchange membrane (AEM) material (Excellion I-200, SnowPure LLC). The surface area of each electrode was 103.2 cm^2 and the AEM material was pre-conditioned in 80 °C distilled water for 24-48 hours.
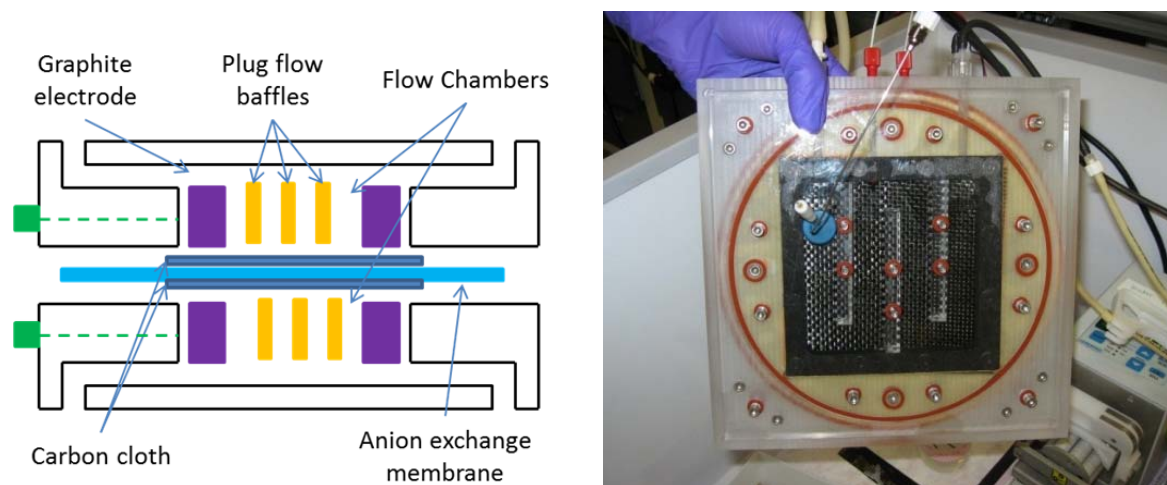

Figure 6 – a) Top view of MFC cross-section, illustrating AEM configuration and two flow chambers as anode & cathode and b) the dual-chamber microbial fuel cell used in this Phase I research.

The performance of this MFC was evaluated with both waste water and pure culture *Geobacter sulfurreducens* to compare the power production capability of each option. Several dual-chamber fuel cells were built to this design to ensure there was no cross-contamination between microbes and to provide multiple test iterations, as required. All tests were run at a consistent temperature of 30 °C.

Geobacter sulfurreducens, strain DL1.
In the pure culture experiments, the MFCs were inoculated with *G. sulfurreducens* strain DL1 (shown in Figure 7) and operated with continuous current production for more than two months. Biofilm/current growth was achieved via three-electrode poising of the anode at +300 mV (vs. Ag/AgCl) at a substrate (acetate, CH_3COOH) loading rate of 16 g/m^2/min. Under the three-electrode scenario, the cathode serves as a counter/auxiliary electrode and the potentiostat

compensates for any limitations at the cathodic reaction—effectively short-circuiting the fuel cell to achieve maximum substrate oxidation and current production. In this configuration, the anode achieved steady-state current production of 2.7 A/m^2 (shown in Figure 8) which equates to 26.1 mA normalized by anode surface area of 103.2 cm^2. As illustrated in Figure 8, there is some variability in the steady-state conditions of biological systems, i.e. the oscillations in i_{max} from hour 193 to hour 303 were due to slight fluctuations in temperature (opening of incubator) or replacing the substrate media bottle.

Figure 7 – a) A microscope view of an anode coated with *Geobacter sulfurreducens* microbe used in the Phase I study.
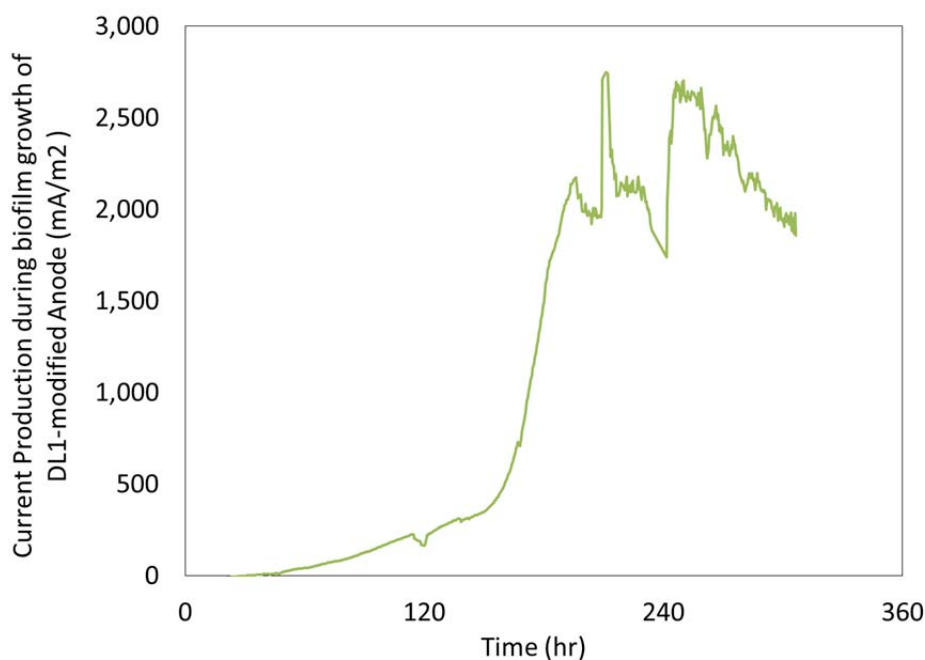
Figure 8 – Current production during biofilm growth of DL1-modified anode.

After initial steady-state values were achieved, current production was manipulated by adjusting the media pumping rate, thus adjusting substrate loading. A maximum steady-state current production of 5.0 A/m^2 (48 mA normalized by anode surface area of 103.2 cm^2) was achieved at an acetate (CH$_3$COOH) loading rate of 410 g/m^2/min and steady-state was sustained through the end of the 54 hour experiment (Figure 9).

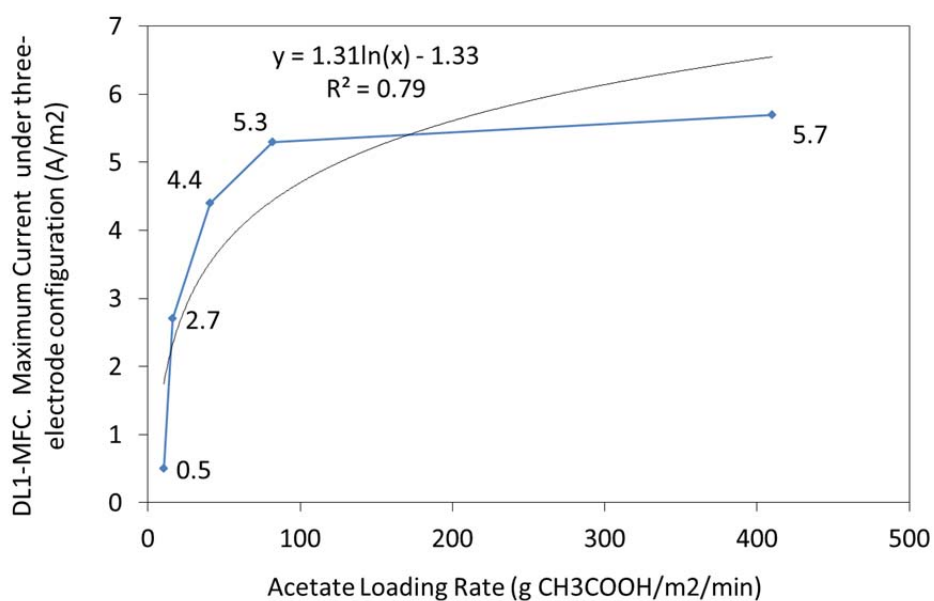**Figure 9 – Relationship between sustained current production and substrate loading rate in DL1-fed MFC under 3-electrode configuration (Ean: +0.3V vs Ag/AgCl).**

Voltage/power production was quantified under two-electrode mode (0.35 V_{cell}) with an aerated water or phosphate buffer cathode. Current/power production was severely limited by the cathodic oxygen reduction reaction (ORR), and produced only ~10 mA/m^2 (net 1 mA). The thermodynamic potential of ORR is > 0.8V vs. a Ag/AgCl reference electrode; however, the circumneutral-pH and mesophilic temperatures required for biological growth in MFCs typically result in maximum cathodic potentials of ~0.3 V vs. Ag/AgCl. This has the effect of reducing the overall cell voltage ($V_{cell} = E_{cath} - E_{an}$) and thus reduces fuel cell output power. Cathodic potentials observed in this DL1 fuel cell (at maximum power production; V_{cell}: 0.35 V) remained below -0.2V vs. Ag/AgCl, indicating a severe membrane/cathode limitation. Replacing the water/buffer catholyte with ferricyanide (16.47 g/L $K_3Fe(CN)_6$) at the cathode increased cathode potential to ~ +0.2V vs. Ag/AgCl and resulted in a maximum current production of 0.83 A/m^2 (8.0 mA normalized by anode surface area of 103.2 cm2), though it could only be sustained through the end of the 18 hour experiment, at which point the majority of the ferricyanide was reduced to ferrocyanide (Figure 10).
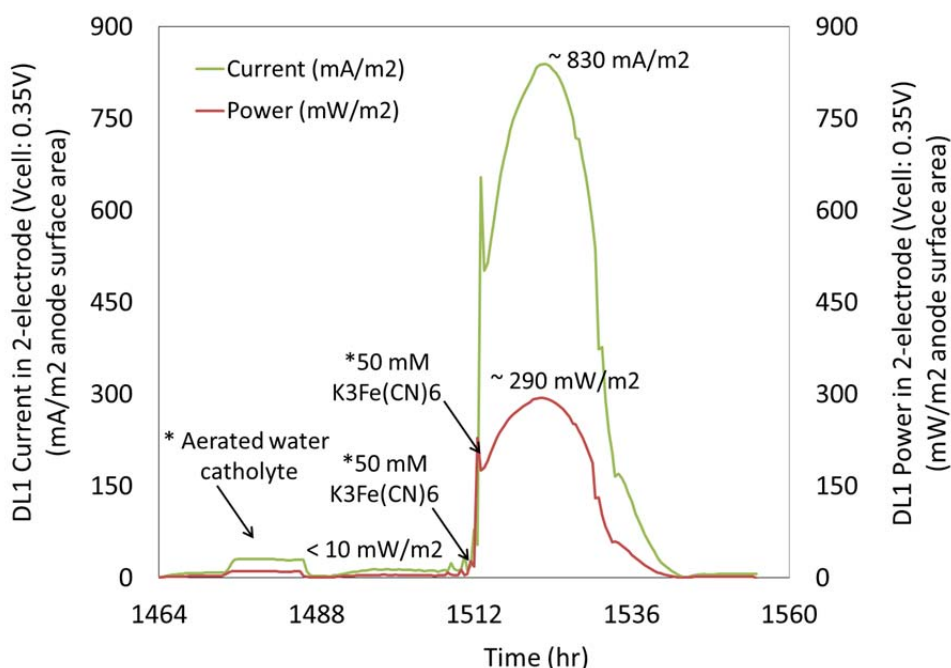

Figure 10 – Current and power production from DL1-MFC under two-electrode configuration, operated initially with aerated water as the catholyte and then with 16.47 g/L potassium ferricyanide (cell voltage of 0.35 V).

Wastewater
In the wastewater experiments, the MFCs were inoculated and fed with high-strength domestic wastewater, and biofilms were similarly grown in three-electrode mode via potentiostat (E_{an} = -200 mV vs. Ag/AgCl). Figure 11 displays a representative growth curve of a wastewater-fed MFC, where the large oscillations observed at maximum current were due to the on-off cycle of a pump supplying the wastewater. The wastewater-modified anodes achieved approximately ½ to 1/3 of the maximum current produced by the DL1-anodes, where i_{max} from acetate-amended wastewater (0.82 g CH_3COOH per L) was ~2.0 A/m^2. This equates to 19.3 mA normalized by anode surface area of 103.2 cm^2. With no acetate amendments, the wastewater-fed anodes

achieved between 0.57-0.80 A/m^2, which equates to 5.5-7.8 mA normalized by anode surface area of 103.2 cm^2. The reduction in current observed after stopping the acetate amendment indicates that the wastewater lacks the substrate levels (i.e. food source for bacteria, such as the acetate used in the pure-culture MFC introduced in the previous section) needed to maximize power production.
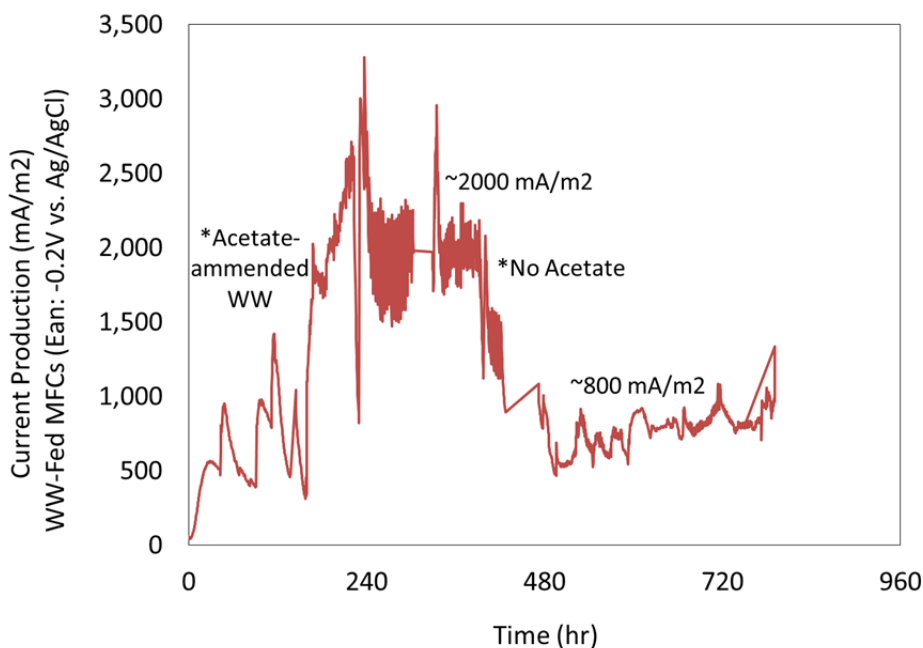

Figure 11 – Representative current production during biofilm growth of wastewater-modified anode (Ean: -200 mV vs Ag/Agcl).

Similar cathodic/membrane limitations developed in the wastewater-fed MFCs under two-electrode configuration (V$_{cell}$: 0.1 V or 0.35 V), and the cathode potential could only be brought > 0 V vs. Ag/AgCl with the use of a 16.47 g/L K$_3$(CN)$_6$Fe catholyte. Polarization of the fuel cell (as shown in Figure 12) was achieved by sweeping the cell voltage from open circuit (OCV: 0.7 – 0.8V) to 0.02V and measuring the response in current and power. Maximum power production from the wastewater-fed MFCs was 138 mW/m^2 (net 1.43 mW).
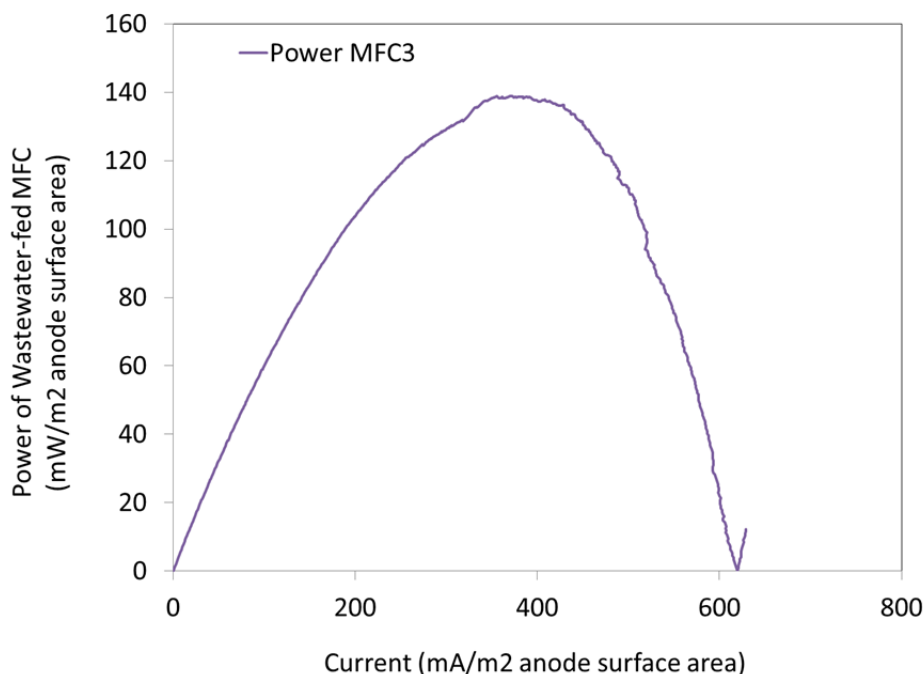
Figure 12 – Polarization of Wastewater-fed MFCs from OCV to 0.02V (v = 0.1 mV/sec).

Conclusions

In three-electrode configuration, both the DL1- and wastewater-modified anodes produced an order of magnitude greater current density than what is typically seen from benthic microbial fuel cells (< 0.1 A/m^2) [9,10,11]. In comparison to BMFCs however, the fuel cells were severely limited by the oxygen reduction reaction at the cathode. ORR in marine environments is facilitated by a higher solution conductivity (i.e. salinity 30,000 uS/cm) and naturally forming cathodic biofilms that catalyze oxygen reduction, which result in sustained cathodes potentials of 0.2-0.4 V vs. Ag/AgCl.

For application to utilizing one of these fuel cells as an electrical charging source for the microrobotic system, the MFC inoculated with *G. sulfurreducens* has shown to be nearly twice as effective as a wastewater MFC at the same volume and under the same conditions. The current output of 8 mA at 0.3 V would suffice as a power system in these initial tests and could be used to charge an energy storage device such as a battery or super capacitor. However, under unconstrained conditions at the cathode, a possible 48 mA would provide six times the power output, thereby reducing the charging time of the energy storage device considerably. To improve feasibility and scale-up potential of these systems, future work should focus on optimization of the cathode reaction (e.g. abiotic, enzymatic, or microbiological oxygen reduction catalysts; quantifying optimal anode/cathode surface area ratios; alternative oxidants such as NO_2^-/NO_3^-).

Low Power Electronics

When considering the low power electronics requirements for the Phase I portion of this research, two areas were specifically investigated: analysis of an energy harvesting circuit, simulation of the power distribution system, and the evaluation of energy storage technologies.

Figure 13 below shows a general electrical model of the entire robotic system. The voltage source on the left represents the MFC, the power converter in the middle represents the energy harvesting and distribution circuits, the capacitor on the right represents the energy storage device and the switch and resistor on the far right represent the output motor.
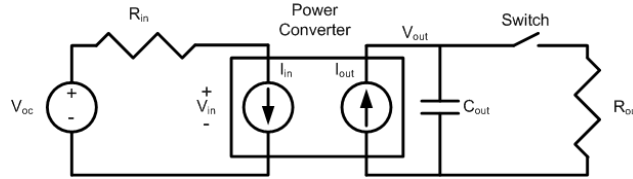

Figure 13 – A top level diagram of entire MFC system based on input voltage, power conversion through energy harvesting circuit, and output through the load (motor).

Analysis Energy Harvesting Circuit

Microbial fuel cells (MFCs) are high-impedance, low voltage energy sources. These output characteristics require an energy harvesting circuit to convert the power to a voltage level into a usable form. The low power levels available from the microbial fuel cells put a premium on the efficiency of the energy harvesting circuit so that less of the power is wasted in conversion. An existing energy harvesting circuit was analyzed and tested to determine its performance and to identify improvements that could be made.

The existing circuit takes in the high-impedance, low voltage source power from the fuel cell and regulates the input voltage to operate at the maximum power point of the source. The operating point is adjusted by the user to match the characteristics of the source, and a value of 0.35 V was selected for this MFC. The output acts as a constant current source and can be used to charge an energy storage device. A shunt regulator limits the maximum voltage of the output to 24 V.

A key component of the energy harvesting circuit is the startup circuit, which uses a zero-voltage threshold MOSFET to create an oscillator capable of running at an input voltage as low as 0.25 V. The oscillator drives the transformer until the voltage on the secondary side is high enough for the control circuit to become active and drive the Primary Side Power Devices. The other secondary side winding on the transformer provides an isolated output for the mechanism. A block diagram representation of the current energy harvesting circuit is shown Figure 14.
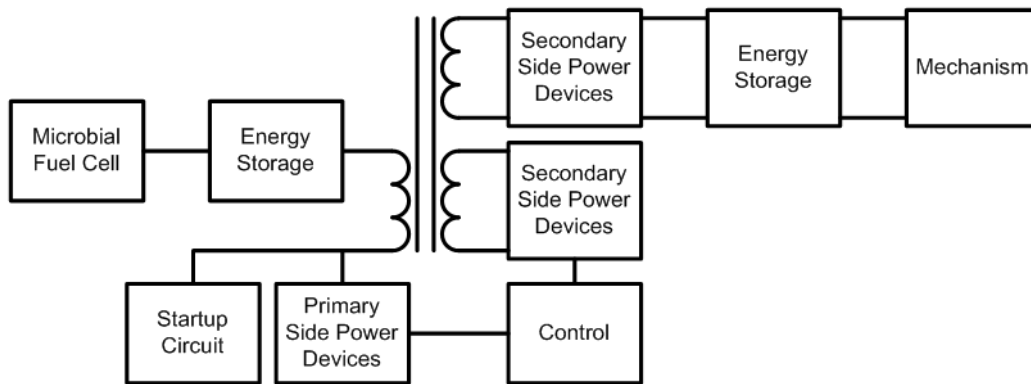

Figure 14 – Block diagram representation of the energy harvesting circuit used in this project.

The existing energy harvesting circuitry uses a complicated regulator design that limits its efficiency, especially at low power levels. Further, the power stage for the energy harvester circuit can be optimized by using power devices optimized to minimize losses. From a system point of view, the size and mass of the energy harvesting circuit also become important as the current energy harvesting circuit requires large capacitors for energy storage on both input and output and complicated and bulky magnetics.

Simulation of the full system electrical model
SPICE simulations of the energy harvest circuit output, energy storage element, comparator, and mechanism were developed to show the performance of the circuit from end-to-end. From these simulations, parameter optimization was used to find a balance between minimizing size of the energy storage device while still providing sufficient power to operate the mechanism.

The challenge of working with a microbial fuel cell is that it is a high-impedance, low voltage source. In order to convert the power produced by the fuel cell to a voltage level that can be used by electronics and mechanisms, an energy harvesting circuit must step up the voltage and then store the power.

Figure 15 shows the output characteristics of a simulated fuel cell used to test the energy harvesting circuit. The curves for the power and current of simulated fuel cell were computed based on the selected power supply voltage and series resistance. The operating point of the energy harvesting circuit was then measured at steady state operation, as noted by the highlighted points on the plot.
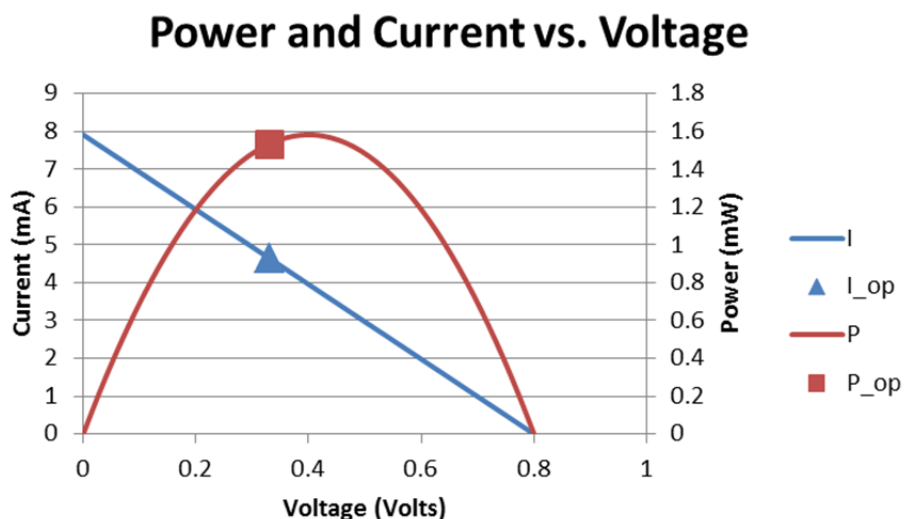
Figure 15 – Output Characteristics of simulated Fuel Cell with Energy Harvesting Circuit operation points.

The output power of the energy harvesting circuit was measured over a range of loads. The peak efficiency was 28% for the source show in the figure above. At heavy loads, the output of the energy harvesting circuit had the characteristics of a constant current source. The circuit produced a constant 58 µA current over a voltage range of 50 mV to 12.5 V. At higher voltages, the shunt regulator begins to turn on in order to limit the output current. The mechanisms being considered all operate below 12 V, so the effect of the shunt regulator was neglected and the

energy harvesting circuit was modeled in SPICE as a current source with the constant value of 58 µA.

Using the test results from the existing energy harvest circuit, a more sophisticated SPICE simulation was developed including the energy harvest circuit output, energy storage element, comparator, and mechanism was developed to show the performance of the circuit from end-to-end. The simulation diagram is shown in Figure 16.
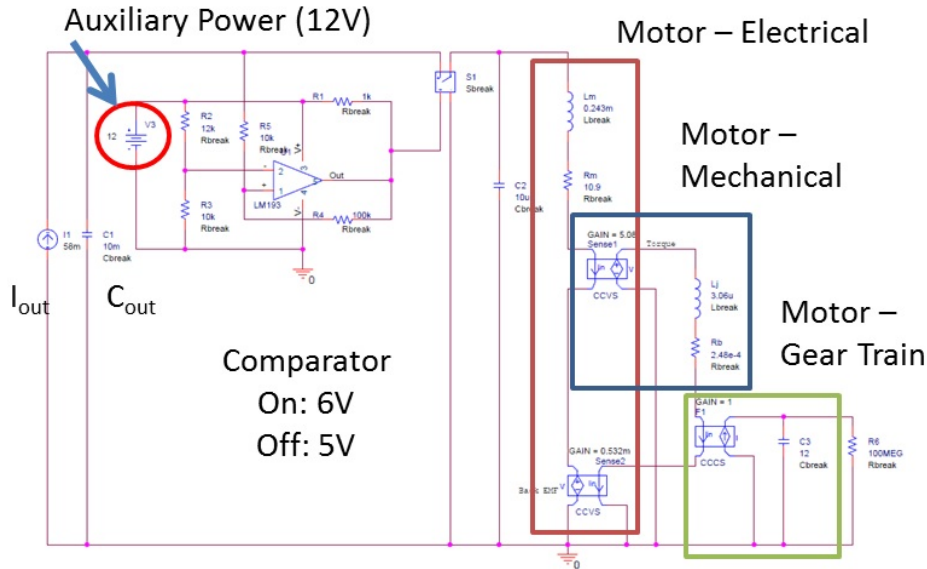
Figure 16 – Diagram of simulated energy storage, power transfer and mechanism drive circuit

From this simulation, the trade between the size of the energy storage element and the operation of the mechanism was examined. As the energy storage element becomes larger, it takes longer to charge to the target voltage, but the mechanism can run for a longer time. The mechanism needs to operate long enough to reach its maximum speed to be effective. These parameters were used to find a balance that minimized the energy storage requirement while still providing sufficient power to the mechanism. The plots in Figure 17 show some of the results for the simulation.

Figure 17 – a) Voltage of the simulated energy storage capacitor, b) motor torque, and c) output motor speed.

The first plot shows the energy storage capacitor being charged by the energy harvesting circuit. When the capacitor reaches its target voltage, the comparator circuit turns on a switch and

powers a 6 V maxon motor available in the lab. The motor remains on as the capacitor charge is drained by 1 V, at which point the comparator turns off the switch. The second chart shows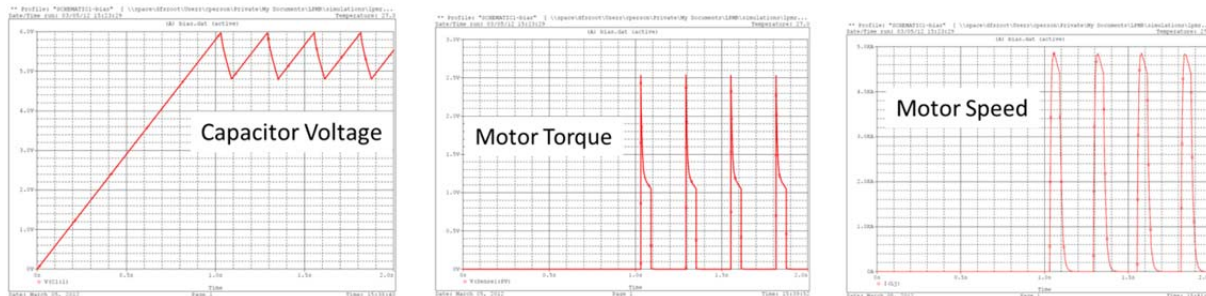 the torque of the motor. The pulses occur when the switch is on. The torque drops quickly as the motor increases speed and a back EMF is generated. The torque also declines as the capacitor voltage drops. The third chart shows the motor speed with respect to capacitor voltage and motor torque. The motor speed ramps up with the initial torque and slows down as the motor's maximum torque is reached. Then, as the voltage (and therefore torque) is no longer applied, the motor speed trails off to a complete stop.

Evaluation of Energy Storage Technologies

High energy densities and low self-discharge losses are important parameters in selecting an energy storage element. The capacity of the energy storage element is greatly influenced by the design of the mechanism, and the self-discharge is dependent on the selection of the type of storage element itself. Four possible technologies are shown in Figure 18: ceramic and tantalum capacitors, super capacitors, and lithium ion batteries. Based on the available charge current and the need to minimize the volume and mass of the energy storage elements, the super capacitors are a promising technology and were used in the energy storage circuit.
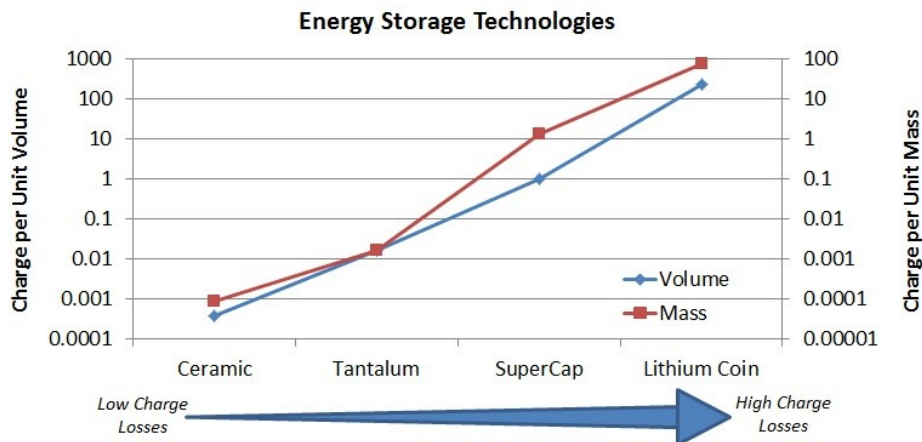
Figure 18 – Storage capacities vs. mass and volume for representative energy storage technologies.

As shown in Figure 18, the energy density of a battery is orders of magnitude greater than that of a ceramic capacitor, so based purely on energy density, lithium ion batteries are the superior technology for storing energy. As another primary consideration in selecting an energy storage technology, self-discharge also increases from ceramic capacitors to lithium ion batteries. Self-discharge needs to be minimized, so for this selection factor, lithium ion batteries are the worst performer. The self-discharge for ceramic and tantalum capacitors is on the order of nanoamps and scales with capacitance value and voltage. For super capacitors and lithium ion cells, both of which are electro-chemical devices, the self-discharge losses are much greater, and for lithium ion cells, can even exceed the available charge current. For super capacitors, the self-discharge current can be a few microamps, which is up to 10% of the available charge current from a power source such as a microbial fuel cell. Based on the available charge current and the need to minimize the volume and mass for the energy storage elements, super capacitors are a promising technology.

Another critical parameter in energy storage element selection is the equivalent series resistance (ESR) of the device. The mechanism requires a relatively large current pulse for a short duration, and if the energy storage element has a high ESR, much of energy stored in the element will be dissipated as heat across the ESR. Ceramic and tantalum capacitors, as well as lithium ion batteries, all have ESRs well below 1 Ohm. However, the first generation of super capacitors had ESRs of up to 100 Ohms. This level of ESR would be acceptable for a low current application, but for a high current, pulsed application, nearly all of the energy would be dissipated in the ESR and not in the load. Recent advancements in super capacitor technologies, such as BestCap from AVX, have reduced the ESR below 1 Ohm and are suitable for pulsed applications. The energy density of these capacitors is less than the traditional super capacitors, but still much greater than for tantalum and ceramic capacitors.

To understand the value in selecting the super capacitor over other technologies, a practical example is warranted. To begin, a simple analog for an eventual robotic implementation was selected: a Hexbug® Nano. The Hexbug® Nano is a small, battery operated autonomous toy bug which locomotes from the combined action of the vibrations induced by an offset motor and flexible legs that are angled to help induce forward motion. The motor power is provided by a coin-cell type battery at 1.5 V and 150 mAh of charge stored. The motor itself has an internal resistance of ~10 ohms.

A capacitor, as intended for this application, is relatively easy to use as a charge storage device and is typically capable of handling thousands of charge/discharge cycles when operating within the device parameters. In order to gauge whether or not a capacitor would be a suitable replacement for the battery, a comparison of the energy storage capabilities for each device type is performed. For a battery with a 150 mAh capacity we have 540 coulombs of charge, where 1 mAh = 3.6 coulombs. Further, the voltage produced by this battery is 1.5 V, which gives (approximately) 810 joules of energy. For a capacitor to provide an equivalent amount of energy, the capacitance would need to be $C = 2U/v^2 = 2(810)/(1.5)^2 = 720$ farads. Table 1 summarizes these calculations, comparing the coil cell battery with an equivalent capacitor. While a capacitor of this size, given the introduction of the super capacitor technology, the physical size of such a device is considerably greater than that of a chemical battery.

Table 1 – Comparison between coin cell battery and the capacitor needed to store the equivalent amount of energy.

		Coin Cell Battery	Equivalent Capacitor
Voltage	(V)	1.5	1.5
Charge	(mAh)	150	
Charge	(C)	540	
Energy	(J)	810	
Equivalent Capacitance	(F)		720
Volume	(mm^3)	570	135000

The largest commonly available ceramic or tantalum capacitors have typical capacitance values in the micro- and nano-farad range. Super capacitors provide the ability to store charge comparable to these small, coin-cell batteries, but in a substantially larger package. The coin cell used has dimensions of 11.6 mm (diameter) x 5.4 mm (height), equating to ~570 mm^3. An available super capacitor of similar charge storage capability measures 40 mm (diameter) x 108 mm (height) - a volume nearly 240 times that of the coin cell battery.

With the charge stored in the coin cell, the representative robot would be able to operate continuously for about an hour. By trading operating time for device volume, a suitably sized capacitor (volume and capacity) is available to allow an MFC-based robotic vehicle to be feasible.

Conclusions

Through the investigation of the low power electronics subsystem, several successes were achieved. From the predicted charge capabilities of the MFC through to the simulated output of a locomotion system actuator motor, an end-to-end system simulation was developed to analyze the capabilities of each aspect of the electro-mechanical subsystems. This simulation was primarily used as a sizing application for capacitor and motor selection, as well as pinpointing areas where efficiencies would need to be made in future electrical hardware development.

Analysis using this simulation showed that an effective amount of power would be distributed from the MFC that could be harvested and used to charge an energy storage device. Simulations also showed how long various energy storage devices would take to become charged to a useable capacity and the determination was made to select a super capacitor for experimental testing.

Preliminary tests conducted with a fully charged capacitor activated an LED to predict the overall output lifetime of the discharge operation. The simulation was then used to show that a small 1.5 V motor could be actuated as well. This was verified with a bench-top test, where a simulated power source charged a super capacitor which was discharged to actuate a 1.5 V motor. The simulation would also then be used for sizing the locomotion system motor based on the mechanical output requirements of the actuator, which will be discussed in the following section of this report.

Throughout the investigation into low power electronics, specific areas and methods were identified where the electronics could be tailored for increased efficiency, primarily in the power harvesting and energy conversion circuitry. Additionally, key electronic components were identified that would vastly decrease the volume of the associated electronics. The most significant of which would be integrating energy harvesting and power regulating IC chips, which would greatly decrease size, weight and power of the low power electronics subsystem.

Biologically Inspired Locomotion

Given the nature of the MFC, a very low amount of continuous power output is available (~2 mW at 0.35 V), which will primarily be dedicated to charging a super capacitor over a period of time. Once the super capacitor has reached a threshold value, it will be discharged to provide power to the locomotion system or desired sensors. The overall storage capability of the super capacitor is not expected to be very high and, even fully discharged, the amount of instantaneous power available will not be significant enough to actuate a device to provide locomotion to the vehicle. Therefore, the team investigated locomotion mechanisms that would allow for the build-

up of mechanical potential energy before unloading it to provide a propulsion movement forward.

Mechanism Considerations
The mechanism requirements for the vehicle locomotion actuator systems being investigated in this project were defined as follows:

Qualitative:
1. A novel low power robotic locomotion system for rough planetary surface
2. Locomotion system requiring low activation cost
3. Reduce or eliminate onboard electromechanical hardware

Vehicle:
1. Approximate mass of entire vehicle: 1 kg
2. Weight of mobility system less than half of total system mass (~500 g max)
3. No volume envelope defined

Environment:
1. Space environment
2. Focus the on surface of asteroid
3. Microgravity: ~1/100th of the gravity present on Earth
4. Thermal impacts not considered in this study
5. Long duration mission

Power Available:
1. 1 mW (0.001 W) constant input of electrical energy into battery/capacitor
2. Max voltage supplied: 12 V (a more realistic number is 3-9V)
3. Output from voltage amplifying circuit is used to charge either battery or a capacitor until capacity reached, and then rapidly discharge to power a motor or any other actuation device.
4. Time to charge capacitor is dependent on size of capacitor. Initially, there was no specified capacitor selected, nor expected time to recharge.
5. Discharging time is not initially specified and will be dependent on power required by motor/actuator.

Locomotion:
1. Novel low power system
2. Considerations: Hopping/Walking/Tumbling locomotion system
3. Ability to be scaled up to be able to control different directions
4. Demonstration of mechanism to control movement in one direction.
5. No speed or cycle rate requirement

Environmental Considerations
Understanding the environment and looking at how its characteristics affect or impede the motion of the mechanism is important. Different known asteroids of various sizes and masses were investigated to get a wide range of gravity and coefficient of friction values. These asteroids include Ceres, Vesta, Europa, Hecktor, Aurora, Flora, Gluake, and 99942 Apophis.

From these, three were down-selected as appropriate targets of opportunity, as they provide a wide range of analysis for this project. Those down-selected and considered in more detailed analyses are Ceres, Glauke and 99942 Apophis and are shown in Table 2.

Table 2 – Asteroid targets of opportunity and environments considered in the locomotion system development.

Name	Ceres	Glauke	99942 Apophis
Diameter (km)	953	35	0.27
Mass (kg)	9.50E+20	3.50E+16	2.70E+10
Mass (Earth ratio)	1.59E-04	5.86E-09	4.52E-15
Surface gravity (m/s^2)	0.279	0.009	0.00011
Gravity compared to Earth	0.028	0.000917	0.000011
Escape Velocity (km/s)	0.51	0.009	0.000144

Ceres is the largest asteroid and one of the five dwarf planet in our solar system, and the only in the asteroid belt. Glauke dimensionally lies between Ceres and 99942 Apophis in diameter and was used as a median option. 99942 Apophis is a near-Earth asteroid that caused a brief period of concern in December 2004 because initial observations indicated a small probability (up to 2.7%) that it would strike the Earth in 2029. Additional observations improved predictions that eliminated the possibility of an impact on Earth or the Moon in 2029. However, a possibility remained that during the 2029 close encounter with Earth; Apophis would pass through a gravitational keyhole, a precise region in space no more than about a half-mile wide that would set up a future impact on April 13, 2036 [12]. Due to the concern of a possible impact and exceptionally low gravitational force, asteroid 99942 Apophis is expected to be a strong target candidate. The near earth proximity allows for easy access upon its arrival and it also has similar characteristics to many other asteroids.

Actuator Designs
Observing the mechanical design constraints and the expected environmental conditions affecting the locomotion system, many characteristics need to be considered. These characteristics include system mass, gravitational environment, contact environment, vehicle size, actuation speed, and actuator complexity. Although all primary areas of investigation for this project are targeted to operate as one complete microrobotic system, the mechanical system is directly related to the electronics system while the electronics system is directly influenced by the microbial fuel cell. This demonstrates how important it is to know both the electrical and mechanical attributes prior to creating a locomotive design for this system.

Two distinct actuators were designed as part of the locomotion system analysis. The first utilized a spring-loaded bi-stable mechanical potential for building up energy for a propulsive "leap" forward when the threshold was reached. The second utilized a rotary motion to lift a weighted "pendulum" before releasing it to cause the spherical body of the robotic system to roll (also considered a "tumbleweed" technique in other robotic studies).

Bi-stable Spring-loaded Actuator

The team investigated various spring-loaded mechanisms as the baseline mechanical actuator for a hopping locomotion system, particularly based upon the visco-elastic properties of biological muscle. Traditional torsional and coil springs were the first consideration for this baseline due to the elastic properties of the materials. Further investigation led the team to consider bi-stable mechanisms, which provide multiple positions of mechanics/structural stability and requiring only a particular force to transition between them. As shown in Figure 19a, exerting a force (F) on a semi-rigid body (of length L) that is held in place by opposing forces (P) will transition the semi-rigid body between points of stability. After the mid-point between these stability points is reached, the semi-rigid body will "spring" towards its next stability point, exerting an instantaneous force (downward in the case of the diagram).
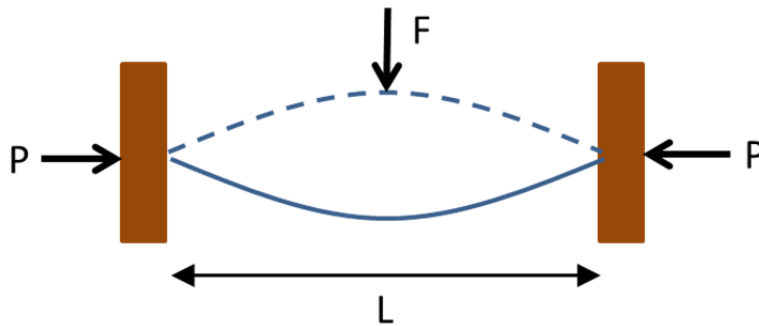

Figure 19 – Free body diagram of a simple bi-stable mechanism.

This theory was then applied to the development of a mechanism that would induce an instantaneous force after slowly building up potential energy. Several development iterations were completed prior to a final approach being selected. A free body diagram of the spring-loaded bi-stable mechanism is shown in Figure 20.
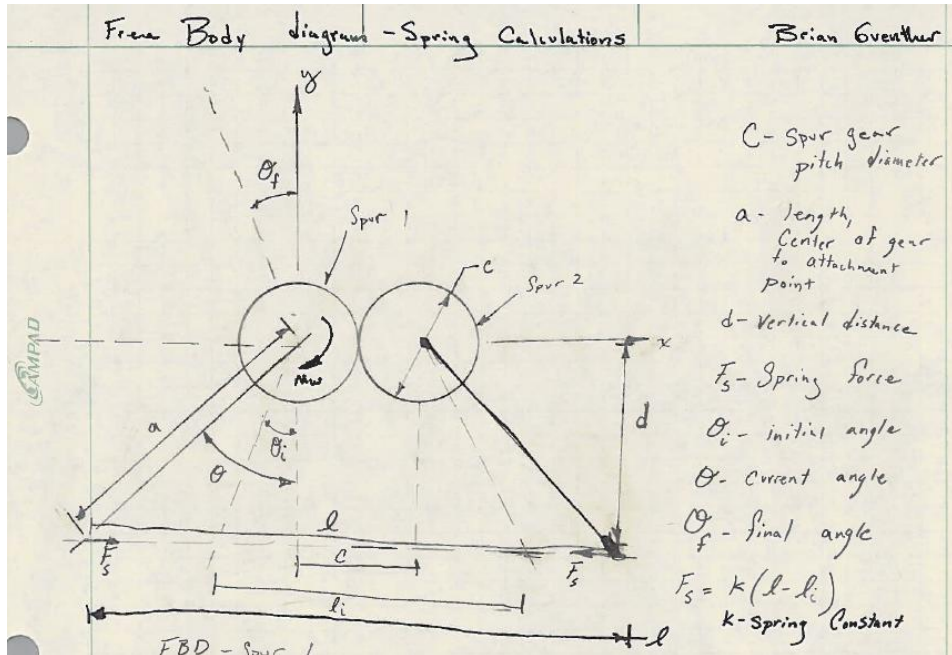
Figure 20 – Free body diagram of the selected spring-loaded bi-stable actuator.

Based on this theory, a detailed design was completed to evaluate the mechanical capabilities of the system. Initial simulations were developed to predict the power requirements to actuate the system, which allowed for fine-tuning the gearing and spring stiffness used in the design.

Two meshing spur gears are held in contact by the rigid body of the system. Attached to each spur gear is an arm that extends away from the center of each spur gear. An extension spring connects the two arms and as the spur gears rotate to bring the arms upward, the spring stretches. Once the arms are in the horizontal position, the spring is at its longest (and strongest) point. As the spur gear rotates slightly past this point, the spring pulls on the arms so that they snap together. Through this motion, the end of the arms impact the ground, imparting a hopping motion onto the mechanism. The major components to the actuator design are shown in Figure 21a while a more detailed isometric view is shown in Figure 21b.

Figure 21 – a) Engineering model of the spring-loaded bi-stable actuator and b) a detailed isometric view of the spring-loaded bi-stable actuator.
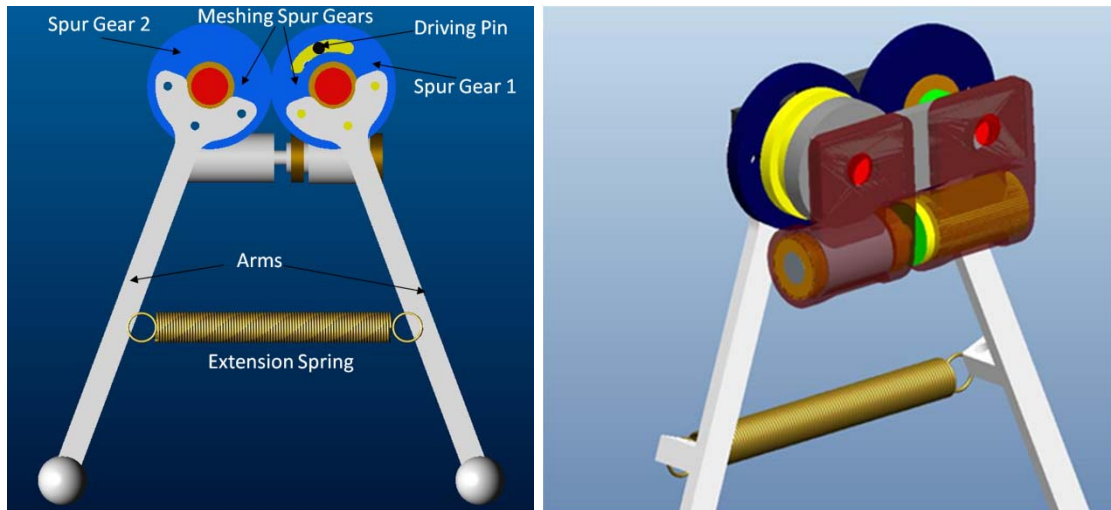
The spur gears are rotated using a gear train that comes off of a small electric motor. Since the spur gears are meshed together, only one spur gear is driven by the motor. The second spur gear (Spur Gear 2) rotates as a result of being meshed to the driven spur gear (Spur Gear 1). Spur Gear 1 is rotated through the action of a pin pushing on the end of a circular slot cut into the spur gear. As the pin pushes on the end of the slot, both spur gears are rotated through the range of motion and the spring is stretched. As the spur gear rotates through its mid-point, the torque created by the spring transitions from working *against* the rotation of the spur gears to *acting in the same direction* of rotation of the spur gears. The torque created by the spring acts to accelerate the rotation of the arms. The slot in Spur Gear 1 allows the gear to rotate unrestrained. In order to actuate the other way, the motor rotates the other direction.

The driving gear train is a worm and worm wheel gear set. The driving pin is inserted into a hole in the pin spacer. The pin spacer is fastened to the worm gear. Small 4-40 (1/8" long) socket head cap screws are fed through clearance holes drilled in the pin spacer and threaded into tapped holes drilled in the spur gear. The pin spacer separates the worm gear and the spur gear so that the worm has the necessary clearance to rotate. The pin spacer also constrains the bearing that is mounted into the worm wheel. The worm gear is attached to the output of the motor and mounted perpendicular to the center axis of the spur gear. The worm wheel and spur gear are mounted on bearings that are pressed onto a stationary shaft. This allows for the spur gear and the worm wheel to rotate independently. Spacers are placed along the stationary shaft to constrain the bearings (shown in green). The two stationary shafts (one along the axis of each spur gear) are mounted into two rails. This forms the primary structure of the mechanism. A cross section of the gear train through Spur Gear 1 is shown in Figure 22.
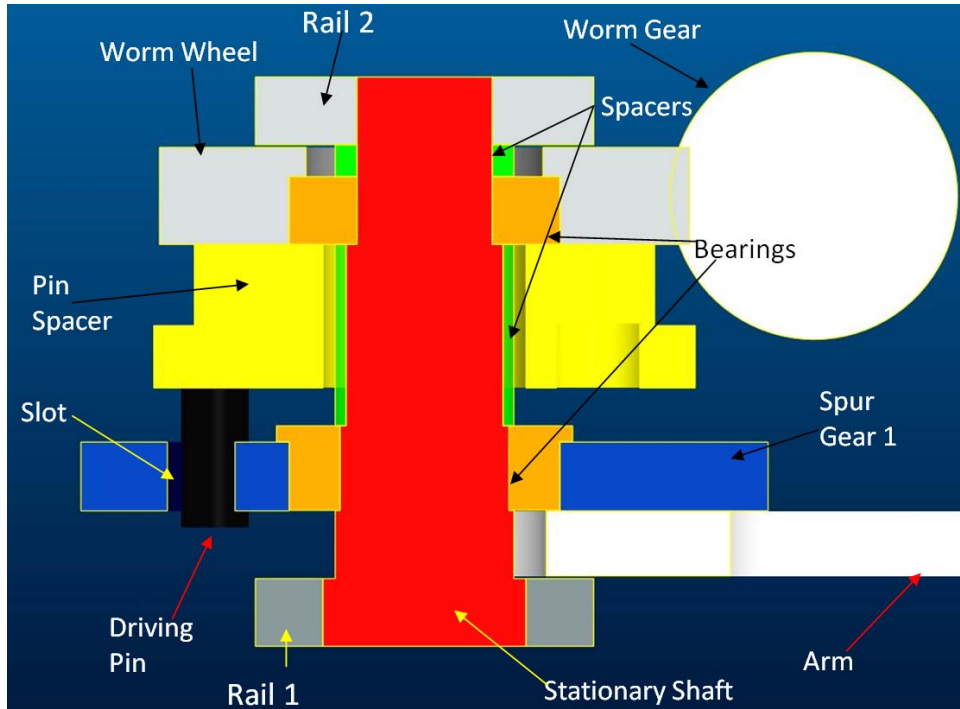
Figure 22 – Cross-section of the gear train for the bi-stable actuator.

A worm and worm wheel combination was chosen for two main reasons. The first is that it offers a high mechanical advantage in a small package. The small motors being considered do not have enough torque to directly drive the spur gears. The second is that it is resistant to being back-driven. Due to the nature of the charging system, it will be impossible to accomplish each actuation with one discharge of the capacitor. Each actuation will be made up of a number of smaller steps. With back-drive resistant gears, progress will not be lost after the motor turns off.

In order to evaluate the efficiency and effectiveness of the bi-stable actuator, a number of mechanical parameters had to be evaluated. The design details of the actuator are shown in Table 3 and defined below.

Table 3 – Table of mechanical values used for the bi-stable actuator.

	Symbol	Value	Unit
Moment Arm	a	0.0635	m
Spring Attachment Offset	h	0.0048	m
Spur Gear Pitch Diameter	c	0.0322	m
Spring Rate	k	0.46	lbs/in
Spring Rate	k	80.55433	N/m
Spring Initial Free Length	L_i	0.0762	m
Initial Angle, Winding	θ_i	0.357	rad
Final Angle, Winding	θ_f	1.570796	rad
Initial Angle, Releasing	θ_i	1.570796	rad
Final Angle, Releasing	θ_f	2.784593	rad

- **Moment Arm:** The moment arm length is 2.5" and is measured from the spur gear axis to the attachment point on the arm.
- **Spring attachment offset:** The spring attachment offset is the distance from the plane of the middle of the spur gear to the mounting point of the spring on the arm. This offset is needed so that the spring can clear the supporting rails when the arms swing through the range of motion.
- **Spur Gear Pitch Diameter**: The pitch diameter of the spur teeth. This distance dictates the spacing of the holes in the supporting rails. The distance between the two holes should be equal to the pitch diameter of the spur teeth. This value was determined by measuring the spur gears found in the storage area of the mechanisms group.
- **Spring Rate:** This is the spring rate of the spring used in the assembly. The spring that was initially chosen is an extension spring with looped ends. The spring rate is listed as approximately 0.46 lbs/in. The spring has a 3" long free length, has an outer diameter of 0.313", using wire diameter of 0.028". The spring's part number on McMaster-Carr supply company is 9654K714
- **Spring Initial free length**: Catalogue value (3")
- **Initial angle, winding:** This is the angle that the arm rests at, measured from vertical (y-axis of the free-body diagram). This angle determined from the free length of the spring and the moment arm length of the arm.
- **Final Angle, winding:** This is the "tip point" of the mechanism. This angle is also measured from the y-axis of the free body diagram and is equal to 90°. This is the same as the initial angle for releasing.
- **Final Angle, releasing:** This is the angle at which the arm comes to rest after actuating. Since the mechanism is symmetrical, this is the supplementary angle to the initial angle for the winding motion.

Table 4 shows the results of the calculations to determine what the overall torque required by the geared motor shaft is for the designed system. This table also shows the values used to convert the torque at the spur gear to the torque required by the output shaft at the motor. A description of each value follows the table.

Table 4 – Determination of the torque required by the geared motor shaft.

	Symbol	Value	Units
Spring Potential Energy		2.75E-01	J
Max Torque, Winding Up,	τ	0.350	N*m
Efficiency of Worm	η_w	0.3	-
Efficiency of Spur Gear	η_s	0.9	-
Worm Mechanical Advantage	MA	50:1	-
Torque required by geared motor output shaft		0.026	N*m
		3.673	in*oz
		264	g*cm

- **Spring Potential Energy**: The total potential energy that is stored in the mechanism just before the flip point. This is found through simple Hook's law and the geometry of the mechanism.
- **Max torque, winding up**: As shown in the free body diagram, the torque on the spur gear is dependent on the vertical moment arm length and the spring force. The torque that the spur gear sees through the rotation does not change linearly because both values are dependent on the angular position. Through the spur gear's rotation, the moment length is decreasing while the spring force is increasing. The max torque value is found by numerically plotting the torque as a function of angle. The max torque can also be found by taking the derivative of the torque and setting it equal to zero.
- **Efficiency of Worm Gear**: Since worm/worm wheel gear trains rely on sliding motion to transmit torque, they are not very efficient. The efficiency of 0.3 was used to be conservative. Though it has been shown that in some cases efficiencies can drop below even this value.
- **Efficiency of Spur Gear:** In general, spur gears are very efficient (usually greater than 95%). A value of 0.9 was selected to be conservative.
- **Worm Mechanical Advantage:** Due to the high reduction, worms have a significant torque advantage over the worm wheels. The worm wheel that was found in the storage area of the mechanisms area has 50 teeth. Since the worm has one tooth (single lead worm), the worm has a 50:1 mechanical advantage over the worm wheel.
- **Torque Req'd by Motor Output Shaft:** This is the torque that is required from the motor output shaft to turn the worm so that the mechanism can actuate. It is found using the gear ratios and inefficiencies listed above: $T = \tau * \dfrac{1}{\eta_W} * \dfrac{1}{\eta s} * \dfrac{1}{MA}$

Some factors were not included in these calculations including the binding effects of misaligned gears, friction due to rubbing gears, ball bearing friction, losses due to manufacturing tolerances of the spring, effects of lubrication on the gear train, flexure and deflection of machined components and the efficiency of the motor.

There are significant limitations on the size of the motor that can be used in this mechanism. Total power coming from the power source is estimated to be 0.001 mW. The voltage is realistically going to be limited to 6 V. Even though this power is going to be stored in a capacitor, the motor must be as efficient as possible. In order to use the maximum amount stored energy, a maxon DC electric motor was selected as a baseline for the preliminary mechanism design. maxon DC motors are high-end motors and are very efficient. The 6 V brushed DC motor in the RE-13 series was selected, specifically model 118425.

A maxon gearhead is required to increase the torque of the motor. According to the motor simulation, the motor outputs 1 mNm of torque. According to the gearing calculations, 26 mNm of torque is required to turn the mechanism. As such, the maxon gear head part number 137151 was selected. This gear head has a reduction of 67:1, so that increases the motor output torque to 67 mNm, which is sufficient (with margin) to turn the mechanism. As the motor simulation becomes more and more accurate, this gearhead might need to be re-evaluated. The goal is to use the least amount of reduction necessary so that the output shaft of the can rotate the maximum

number of times. Actuation times can decrease if more revolutions are extracted from the gearbox with each discharge of the capacitor.

The electro-mechanical simulation introduced previously in this report (shown in Figure 16) was used to simulate the behavior of the selected DC motor associated with the current available from the simulated discharge circuit. Details of the mechanical motor parameters were added to the simulation from the technical specification sheet for the RE-13 series motor. The results of this simulation are shown in Table 5.

Table 5 – Evaluation of the motor output response.

	Value	Units
Time of Discharging	0.06	s
Speed of motor	5000	rpm
Motor Rotations	300	rev
Gear box Reduction	67:1	-
Worm Wheel Reduction	50:1	-
Number of Teeth of worm wheel rotated	0.090	-
Total number of discharges to actuate	217	-
Time to charge	180	s
Total Time to Actuate	651	minutes
	10.86	hours

The simulation shows that the actuator will be activated for 0.06 seconds for every charge (estimated charge time is 180 seconds). Based on the motor specifications and gearing used, it is expected to take 217 actuations of the motor to reach the stability point of the bi-stable mechanism before the actuator "springs" forward to locomote the vehicle forward. Given these parameters, it is expected that, with the estimated microbial fuel cell discharge rate and the time to charge the energy storage system, the vehicle can move once every 10.86 hours. Although the movement of planetary surface vehicles is designed be slow and calculated, this is a much longer actuation time than would be preferred for an active mission. There are methods that can make this process more efficient, primarily focused around improvements to the efficiency of the fuel cell and the mechanical system. These will be evaluated in more detail in a future study.

Gravitational Pendulum Actuator
For the second actuator development, a different approach was taken. The criteria for development remained the same, but the approach used was more vehicle-wide instead of focusing specifically on the actuator itself. In this design, a mass on a moving "pendulum" at the center of the vehicle body was designed and evaluated to locomote the microrobotic system.

First, a schematic of how the 1 kilogram vehicle would look and operate was made. Ultimately, a spherical design was selected to use a sphere's natural tendency to tumble. The design involves a motorized rigid pendulum that allows an input torque to rotate a pendulum along one axis. The reaction of the pendulum should allow rotation of a bar in only one direction that supports the pendulum. In other words, the pendulum rotates freely upon the motor input torque but slows down during its return due to reactions from a braking system in the support bar and eventually come to rest due to gravity. The rotation of the support bar would also rotate the sphere through a

rigid connection. If additional torque is needed, the motor can be rotated in the opposite direction to assist in the rolling of the spherical vehicle. Figure 23 shows a schematic of how this system would operate.
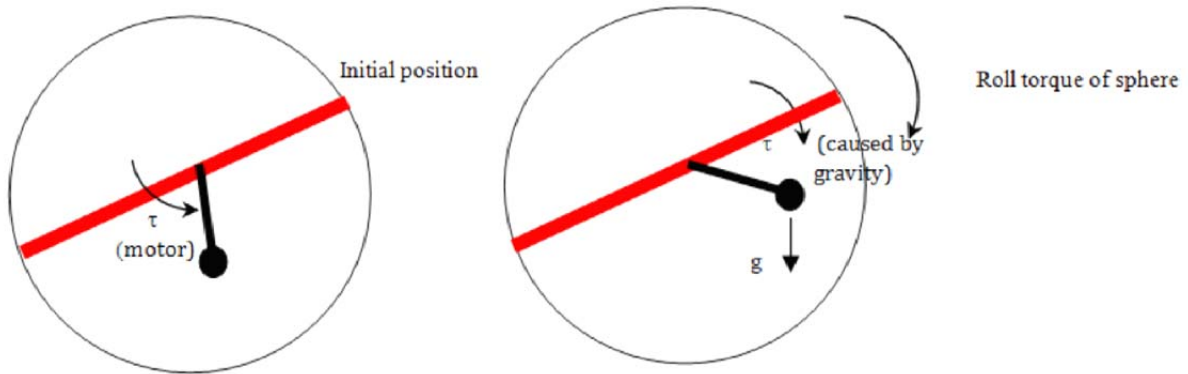

Figure 23 – Locomotion concept of spherical device induced by pendulum motion.

Due to the minimum power input that will be charging and powering the actuator, the accelerations and torques found would enable a proper selection of a motor to power the rotation actuator. Procedures were followed for designing a mechanism, finding a motor and relating those specifications to the electrical components. Once the first iteration of the design was completed, it was discovered that the mechanism did not have enough energy to support its functions. The process was then followed in reverse order to make sure all the different fields function together. This process would include selecting a motor first based on the mechanical response required to locomote on an asteroid surface, then finding the torque ranges needed for the actuator, and lastly creating a design from these specifications.

To find what motor acceleration is needed to overcome the frictional force of the 1 kg robot on the asteroid surface, one must set the friction force equal to the rolling force to the sphere device and create a reaction torque greater than this value. Traditional rolling friction was considered based on a high surface friction value of the asteroid terrain. Actual surface material, roughness, and obstacles were not considered in this investigation. Given the target asteroids under consideration during the project, the rolling torques must be exceeded by the vehicle to allow locomotion on the surface are summarized in Table 6. Obviously gravity is the most significant factor in this analysis, resulting in a wide range of results to consider.

Table 6 – Surface rolling torque to be surpassed to achieve rolling locomotion.

	Ceres	Glauke	99942 Apophis
Vehicle Weight on Surface (kg-m/s^2)	0.279	0.009	0.00011
Frictional Force of Surface (kg-m/s^2)	0.2232	0.0072	0.000088
Frictional Torque to Overcome (kg-(m/s)^2)	0.04981	0.001607	1.964E-05

Observing each asteroid, an investigation was conducted into the optimal motor for functionality with the electrical energy available, the torque load and the torque speed. Also since the mechanism will be operating in a space environment, temperature needs to be considered. Inputting these values into a selection program designed by maxon motors produces a list of

motors from their inventory that can perform the task with the most efficiency. Figure 24 shows the motor options that met the required criteria to roll on the surface of Ceres.
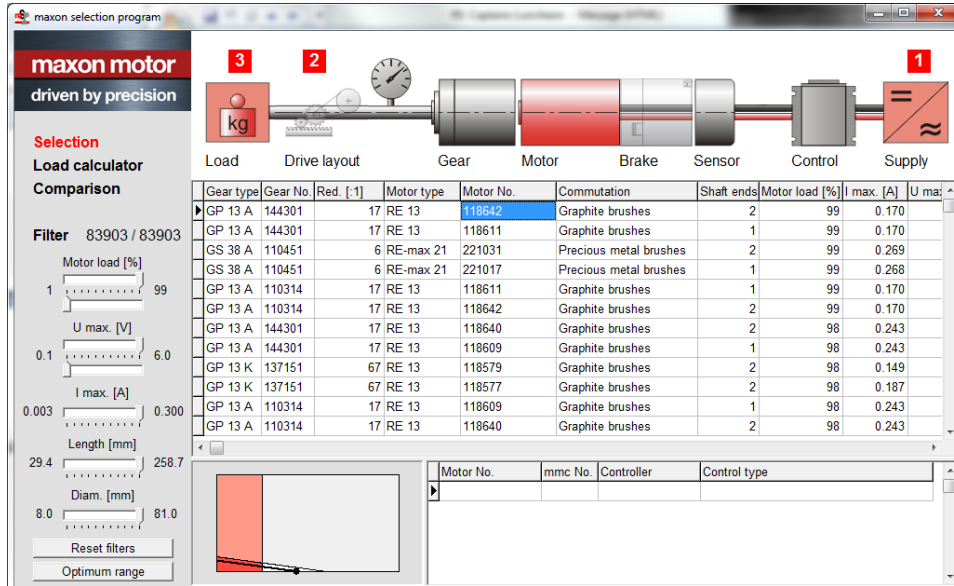

Figure 24 – Down-selected motor options for the mechanism on the Ceres asteroid.

A trade study was conducted on the down-selected motors under the conditions of each asteroid and the motors with the highest motor load were found to be the most appropriate to achieve mission success. Table 7 summarizes the motors selected based on the asteroid torque requirements.

Table 7 – Motor selection based on output torque required to move on each asteroid surface.

Asteroid	Ceres	Glauke	99942 Apophis
Motor	RE-13 118642	A Max-12 265376	EC-6 310599
Torque (Nm)	0.0498	0.001607	0.0000196

The characteristics of these motors were analyzed for an energy performance and parameters such as terminal resistance, terminal inductance, speed constant, torque constant, input voltage from the harvesting circuit, rotor inertia, and speed torque gradient were simulated in the LT Spice simulation introduced previously (and shown in Figure 16). The full circuit analysis was done with recharging two different capacitors, a 22 mF and a 500 mF capacitor. An example of this evaluation is shown in Figure 25 for the maxon RE-13 motor with a 22 mF capacitor actuating on Ceres.
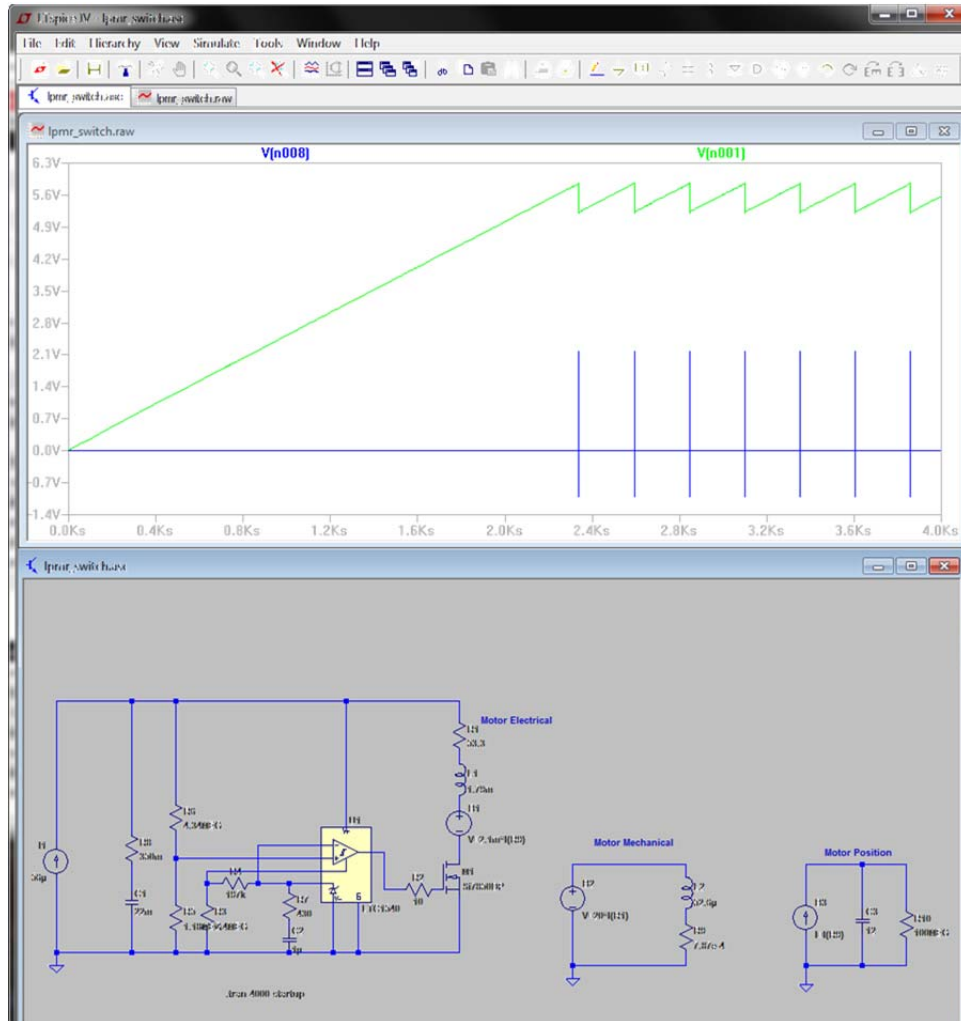
Figure 25 – Electrical analysis of the maxon RE-13 motor operating from a discharged 22 mF capacitor on Ceres.

This analysis would also show the system capabilities utilizing energy storage devices with significantly different capacities. In the above example, an initial recharge time of 2330 seconds is required to bring an initially uncharged capacitor up to a 6 V charge before discharging to the 5 V level and repeating this cycle for the duration of the actuation. The LT Spice circuit would show how much time it takes to charge, the time between operations, the time of action, the charging and discharge of the capacitor, and the speed of the motor for each capacitor and motor combination. Table 8 shows the total start-up and actuation time for the motors selected for each asteroid, as well as the recharge time required for each capacitor.

Table 8 – Capacitor analysis for the motors selected for each asteroid surface.

Asteroid	Ceres	Glauke	99942 Apophis
22mF Capacitor			
Start up time (s)	2330	2330	2330
Start up time (min)	38.8	38.8	38.8
Time of action (s)	0.183	0.108	0.228
Recharge Time (min)	4.21	4.1	4.23
500mF Capacitor			
Start up time (s)	53080	53080	53080
Start up time (h)	14.7	14.76	14.76
Time of action (s)	4.3	2.5	5.2
Recharge Time (min)	96	93.3	96.6

These results show that in all cases, the charge time for the larger capacitor is far more significant than the smaller capacitor, although the operation time is much longer. Depending on the mission's requirements, these extremes or an option in between will be selected to maximize operation time.

Once the motor sizing analysis was completed, the construction of the actuator model was simulated. Simscape, which is software developed under Simulink and Matlab, is a modeling software package in which models are created based on individual components inserted. In the initial analysis, an investigation into how the torque inputs from a motor and gravity on the pendulum affect the output torque on the support bar. Then, the input torque needed for optimum motion and control of the pendulum system was determined. Finally, the output torque of the support beam and its effect on the spherical vehicle body would be analyzed. Figure 26a shows the block diagram used to create the mechanism and the output model of this weighted "pendulum" is shown in Figure 26b.
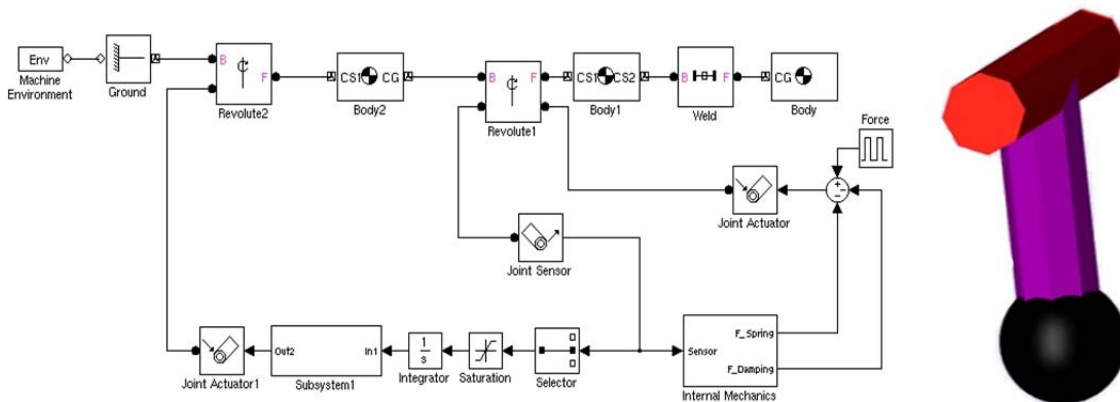

Figure 26 – a) The block diagram of the actuator simulation and b) the actuator model developed in Simscape based on the block diagram.

At the core of the design simulation is the horizontal support bar that is connected to the ground block. The ground block is the origin for the system. Environmental parameters such as gravity were also configured in the system environment block based on the target asteroid. Once the body was constructed, forces or motion profiles can then be added to the joints connecting the bodies to provide movement. Specifically, this design sets the pendulum horizontally which is not at rest. A force is applied to the pendulum to begin the movement through a joint actuator. In order for the support bar to detect proper movement, a joint sensor feeding from the pendulum rod reads the movement in terms of motion. This movement sensing is determined by a joint sensor (from Revolute1) feeding data signals through a series of dynamically natured blocks (Selector, Saturation, Integrator, Subsystem1) to a joint actuator (Joint_Actuator1). Subsystem1 is composed of a vector containing the differential equations used to describe motion through acceleration, velocity and position, which provides motion to the support bar. Also included in the system is the Internal Mechanics block which allows the system to undergo damping and spring effects as the movements of the bodies continue over time. This feature affects the data through simulation in a loop which enables the support bar to act as a braking system bringing the mechanism to rest. The final result showed a moving pendulum bar under the target asteroid gravitational environment would provide an output torque sufficient for surpassing the frictional forces on the spherical vehicle.

A brief study comparing linear actuators and motors was also performed in order to have a wider variety of possible solutions or possibilities for later development. It was found that, although the linear actuators produce little power, they operate quicker than the rotary actuators do. Due to the rotary motors slow but powerful actions make both options desirable under different circumstances.

Conclusions

When considering the design of the mechanical system, there are major precautions that need to be understood prior to the creation of its design. In the case of this project, the most critical aspect of the design process is focusing on all systems being energy efficient. The team also felt that it was important to consider utilizing small movements at more regular intervals to allow for quicker recharge times. This approach was at the core of each mechanism design, as the small electrical charge was used to build up mechanical potential energy. Initial movement to overcome static friction will be higher than overcoming kinetic friction. The motion of the spherical locomotive actuator was derived from observing the mechanism under static analysis while the bi-stable actuator was only affected by static conditions. Energy regenerative movements could also be considered to offset the capacitor charge time in both cases, but this was not considered in this early phase research project.

Due to the large amount of time needed to operate the system, further analysis of the electrical components was done. Looking at each individual component to observe how they affect the whole system was important in understanding what is needed to provide more power to the locomotive aspect of the project. From the characteristics of each component it was shown that having a higher voltage, terminal resistance, torque constant, speed torque gradient, and capacitance are vital to receiving optimal power requirements for any locomotion mechanism. Additionally, the capacitor is the most critical element in this harvesting circuit and has the most impact on the capabilities of the actuator. A larger capacitor increases operation time (discharge time) but also increases the charge and consecutive operation wait times. Serious consideration

needs to be put to toward the energy storage selection for the end-to-end system in order to get the optimal operation time while not increasing the charge and consecutive operation wait time beyond reasonable levels.

Although both actuator designs operate differently, both require hours of charging to produce full actuation and movement. Ultimately the spherical locomotive device requires less energy and operation wait time, but the difference is not significant. From this observation, it was concluded that neither actuator design was optimal for the electrical conditions offered by the MFC at the size limitations they were designed to. The MFC does not produce enough energy to allow for adequate motion in a timely manner for either system. Therefore, from the locomotion system perspective, the system will need to be made more efficient or a lesser output torque will need to be required in order for this to be effective. As such, consideration of a simplified and smaller system will be taken into account for the final end-to-end test to determine if actuation of an electromechanical system at a much smaller scale is possible.

System-level Advancements

Throughout the NIAC Phase I project, the team has advanced the understanding and state-of-the-art of low power microrobotics. The advances within each of the subsystems (microbial fuel cell energy generation, low power electronics, and low power locomotion) have been expressed in the sections above. However, the greatest advances from these technologies come from integrating the capabilities of these subsystems into an end-to-end system.

Figure 27 – A theoretical concept of a microbial fuel cell powered microrobotic system (Credit: K. Reilly/NASA NIAC).

A simulation of the end-to-end system has been performed utilizing the technical specifications and capabilities of each sub-system. This simulation starts at the electrical output of the MFC though the charging potential of an electrical energy distribution controller to the discharging of

the stored energy into a model of the designed actuator. The overall electrical power consumption and mechanical power output has been modeled and are currently being analyzed to improve on each of the subsystem capabilities. Refinements to the energy distribution electronics and the mechanical actuator enhanced the overall mechanical power output and minimized the energy requirements of the system.

Utilizing the results of these simulations, an end-to-end hardware test was performed in the final period of performance of the Phase I research. In this final test, the benthic mesocosm sediment tank (shown in Figure 28) in the littoral lab of the Laboratory for Autonomous Systems Research (LASR) was utilized instead of the dual-chamber fuel cell. This is due to the microbe colony in the dual-chamber fuel cell not being fully inoculated at the time of the final end-to-end system test. The steady state output voltage and available current of the benthic mesocosm fuel cell was shown to be nearly the same as the low volume cell (9 mA in the benthic mesocosm fuel cell compared to 8 mA in the dual-chamber fuel cell).

Figure 28 – a) Sediment-based microbial fuel cell in the Laboratory for Autonomous Systems Research (Credit: J. Hartman/NRL).

For the final experiment, a Hexbug® Original hexapod walker was used as the robotic locomotion system. This version of the autonomous toy bug uses two 3 V DC electric motors to drive six-legged motion from two 1.5 V coin cell batteries. The coin cell batteries were removed and replaced by wiring a super capacitor in series with a knife switch for jitter-free operation. In a future version of this experiment, the knife switch would be replaced by discrete circuitry to allow for self-regulated charge/discharge cycles. An oscilloscope was also integrated into the circuit to evaluate the current and voltage characteristics during the charging and discharging cycles. The full electro-mechanical breadboard system is shown in Figure 29. An additional image can be found in Appendix A and a video of the final test was also taken and available by request.
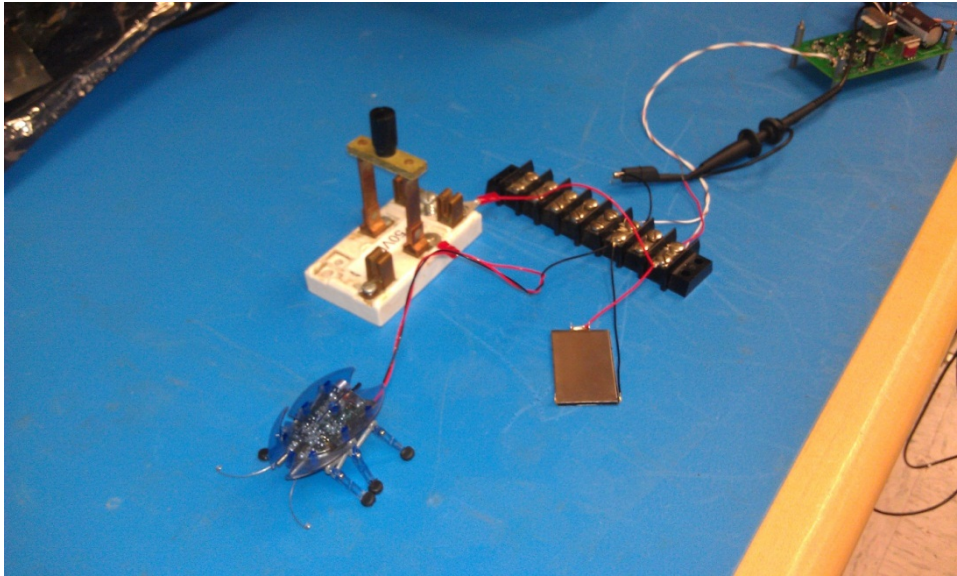
Figure 29 – The test bench setup for the end-to-end test, including (from left to right) the robotic locomotion system, control switch, super capacitor, wiring block, and energy harvesting circuit (oscilloscope not shown).

Upon application of power from the MFC, the charge converter began to supply energy to the super capacitor, increasing the stored energy. The super capacitor started at no charge and after nearly 2 hours, the targeted terminal voltage (3 V) was reached. To discharge the super capacitor, the knife switch was manually closed. This resulted in power being applied to the dive motors of the hexapod robot. The charge cycle for this end-to-end experiment was ~2 hours with a 9 mAh trickle charge from the microbial fuel cell. The total discharge cycle resulted in 13 seconds of motor activity for the robot as the super capacitor discharged the stored energy. It was also evident after ~5 seconds that the motor was not running at the maximum rate and slowed quite considerably by the 10 second mark, showing that the voltage remaining in the capacitor was dropping. This cycle was repeated several times with similar results. The discharge curve of the output voltage from the super capacitor to the drive motors during one test was captured in Figure 30.
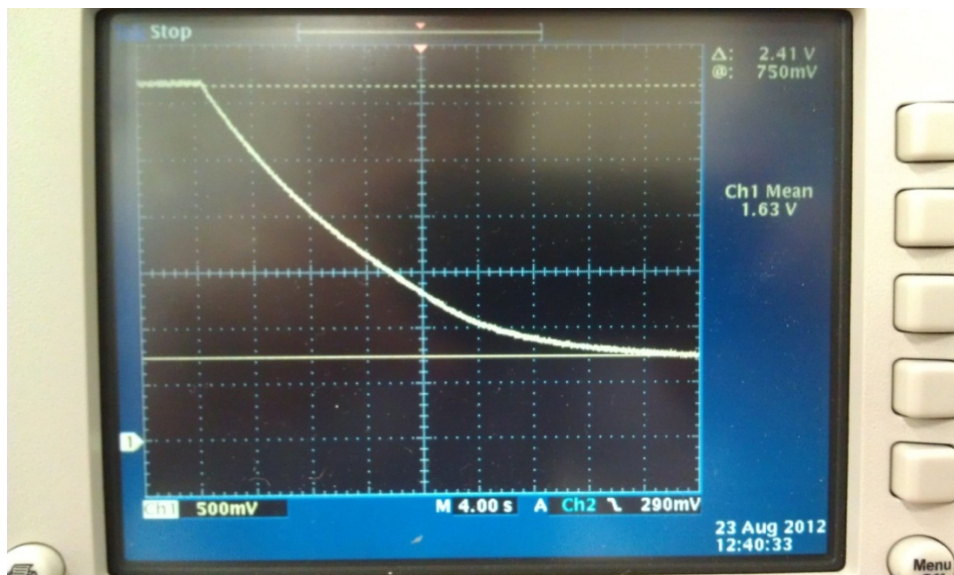
Figure 30 – Discharge circuit voltage of the super capacitor to activate the locomotion motor in the robotic system.

Conclusions

The end-to-end bench-top test was the final step of this NIAC Phase I project. This experiment proved that a microbial fuel cell could be utilized for power generation and that it effectively charges a super capacitor through an energy harvesting circuit, which would be discharged to activate a microrobotic system. Although a benthic mesocosm fuel cell was used for this test, its operative power output is nearly equivalent to the much smaller dual-chamber pure culture microbial fuel cell. The electronics proved to be adequate to harvest the energy of the fuel cell without significant inefficiencies or power losses. The 3 V motor in the robotic locomotion system was operational though this test to allow the robot to take several steps over a short period of time.

Phase I Accomplishments

As noted in the previous sections, there were many strong results from this project, both at the sub-system level and at the system-wide level. Through following the three dedicated research streams and integrating them together for a final end-to-end systems test, several significant results were achieved. These results opened the door to several new questions and research directions that would be addressed with future investigations. Through the duration of this research project, the initially proposed milestones were all achieved successfully and are detailed below.

Milestone 1: Conduct an initial study into various low energy mobility systems and a design a proof-of-concept to be built from the most appropriate option:

A detailed study was conducted on two very different mobility actuation systems: a spring-loaded bi-stable mechanism and a gravity-assisted "tumbleweed" mechanism. Both systems were analyzed mathematically and simulated in a computer environment. In both cases, there were some concerns with the complexity of the engineered systems and

the project came to an end prior to each system being tuned to improve these characteristics. Therefore neither full mechanism was prototyped, however, motors similar to those sized for the systems were utilized in experimental tests.

Milestone 2: **Perform a selection of the required baseline electro-mechanical hardware (if any) for locomotion with an effort to minimize power requirements:**

Both locomotion mechanism designs baselined lower power electro-mechanical motors with limited gearing to reduce power consumption and gearing inefficiencies. Motors selected for both designs were analyzed. A smaller motor was utilized in the end-to-end systems test to demonstrate the capability of powering the motor for a period of time based on the charged super capacitor.

Milestone 3: **Investigate off-board power management electronics to be designed and prototyped to control charging of onboard capacitors/cells from the MFCs:**

Power management electronics were used primarily within the energy harvesting circuit to take in the low power trickle from the microbial fuel cells and then translate it to a manageable voltage. The output power was then utilized to charge the super capacitor.

Milestone 4: **Investigate on-board scheduling management to provide power to locomotion system and associated hardware when needed:**

A charge and schedule management system was investigated for discharging the super capacitor to the locomotion actuator. In the final hardware test, an on-off knife switch was utilized for simplicity to prove the capability of the system. However, a cursory investigation into active electronics to control the discharge scheduling was also completed. The utilization of microprocessors for this activity would be power intensive, which would have to be covered by the MFC. Some lower power microprocessors could be considered when additional sensors and communication subsystems are included in the overall vehicle system, as an approach to determine how to disseminate power to the various devices will need to be considered. Lower power logic gates were also considered and may be utilized in a future benchtop test of a simple schedule management system.

Milestone 5: **Consider existing MFC infrastructure to study the energy profile of the microbes to select the most appropriate microbe for this application:**

Two microbial systems were investigated in the dual-chamber fuel cell to determine which was more appropriate for this application. The first was utilizing the variety of microbes that exist in waste-water and the second was pure culture *Geobacter sulfurreducens*. Through the initial research in a dual-chamber MFC, it was determined that the *Geobacter sulfurreducens* produced nearly twice the power output as the waste-water microbes.

Milestone 6: **Utilize an off-board closed-loop pure culture MFC to provide power to the electronics and controller hardware:**

In the final end-to-end systems test, a microbial fuel cell was utilized as the power generation subsystem to charge a super capacitor, which was then discharged to active

the locomotion system of a microrobotic system. Although the pure culture MFC was not available at the time of the final test due to the colony not being ready for inoculation, it had been shown during this study to provide nearly the same power output as the benthic mesocosms used in the final hardware test.

Milestone 7: Propose methodology for minimizing MFC hardware infrastructure while maintaining acceptable power output levels:

There are several ways that research towards reducing the MFC hardware infrastructure and improving MFC efficiency can be initiated. The first includes ongoing research in the Laboratory for Microbial Electrochemistry towards improving fuel cell efficiency. This includes improving the efficiency of the cathode reaction, as well as research to improve the efficiency of ions travelling through the dual-chamber membrane. Research into micro-fluidic pumps is an upcoming research direction in the robotics group for use as actuation mechanisms, which may also have application for reducing pumping requirements for the MFC infrastructure. Additionally, integrating a pumping system directly with the actuation mechanism in a future iteration of this research has also been discussed.

Milestone 8: Propose a sensor suite to support the system, with consideration of sonar/camera, chemical/biological detection, data transmission, and other low power sensory capabilities:

An initial look into sensor options was done as part of the initial locomotion actuator design. No formal selections were made for specific sensors to support a vehicle, because it was decided early on that the sensors would be mission-specific and geared towards the explicit goals of that mission. However, in general, most existing off-the-shelf systems required more power than was available in addition to the mechanical requirements of the designed actuators. Further investigation into mission-specific low power sensors will need to be conducted under a future extension to this research.

Milestone 9: Test the proof-of-concept locomotion system with off-board electronics and off-board MFC to examine the system potential:

In the final end-to-end systems test for this project, an off-board microbial fuel cell and off-board power electronics were utilized to locomote a microrobotic system on a test bench at the Naval Research Laboratory. The initial proof-of-concept locomotion actuators designed for the project were geared towards a 1 kg vehicle and proved to be too power intensive for the current state of development of the small dual-chamber microbial fuel cell used in this research. Therefore, a smaller robotic system was successfully utilized that was more appropriately sized for the existing MFC.

Project Conclusions and Future Work

Through the duration of this project, the research team had many achievements. The most significant of these achievements was proving that a microbial fuel cell could be used as a power generation subsystem to locomote a microrobotic system. This was shown not only in simulation, but proven through an end-to-end systems test at the Naval Research Laboratory. This was a considerable accomplishment under the NASA NIAC Phase I program.

However, this technology is far from ready for daily use. Future research must be accomplished in order to strengthen this technology and improve the technology readiness level to eventual field use. Future directions for this work lie in each of the three primary research areas: microbial fuel cell energy generation, low power electronics, and low power actuation and locomotion.

In the field of microbial fuel cells, research must be conducted reduce the system size while improving power output. Large pumps must be reduced or eliminated to make this technology appropriate for mobile systems. Efficiencies in membrane and electrode technology are already being investigated at the Naval Research Laboratory, but more attention will be needed in this area in the future. Investigations into eliminating the filters that process spent fuel and oxidant through the development of a complete ecosystem where these spent reactants are the primary inputs for another microbial reaction should also be performed. Additionally, as these systems progress to future uses in space, it is also essential to investigate microbes that could survive the radiation environment of space.

In the field of low power electronics, research must be conducted to further improve the efficiency of the microelectronics used to harvest and distribute power within the system. An investigation into low power microprocessors or digital logic systems for onboard power management should be conducted to allow active charge and discharge scheduling processes. From a materials perspective, improvements in electro-chemical technologies to lower self-discharge losses will increase the charge potential of these devices while reducing overall energy storage volume.

In the field of low power locomotion, research must be conducted to more effectively channel electrical energy to activate an actuator. A more efficient approach to mechanical potential energy storage is also required to improve the overall efficiency of the locomotion system. This includes the use of more efficient electro-mechanical actuators, either linear or rotary motors. A more detailed analysis into a low gravity surface locomotion system is also necessary to ensure an optimal design for this environment.

As a benchmark of the global interest in this research, significant press coverage has been received following an NRL Press Release of information related to this project [13]. There were over 50 reprints stemming from this release, with the most significant press coverage through Wired Magazine (both US and UK), Popular Science, Huffington Post and local ABC TV News coverage in San Francisco. Further interviews were given with German Public Radio show "Current Science", Innovation News Daily (for publication on Space.com and others), and BBC News in the UK. Worldwide interest in the capabilities of both low power electronics and biologically-powered robotic systems is strong, and further advances in this research will continue to generate even more public interest in this topic.

The future achievements of this technology could change the way researchers approach energy growth processes and drive science in a new direction. This can lead to the concept of a perpetual ecosystem which could be used in establishing regenerative power systems for human habited space stations or unmanned robotic systems on planetary bodies. More research is needed in each of these areas in order to bring about these advancements, but this NASA NIAC Phase I research has opened the door to developing novel low powered microrobotic systems fueled by microbial based energy generation.

References and Citations

1. Tasker, F., Henshaw, C. G. (2008). "Managing Contact Dynamics for Orbital Robotic Servicing Missions." AIAA Space 2008 Conference and Exposition. San Diego, CA. 09-11 September 2008.
2. Henshaw, C. G., Healy, L., Roderick, S. (2009). "LIIVe: A Small, Low-Cost Autonomous Inspection Vehicle". AIAA Space 2009 Conference and Exposition. Pasadena, CA. 14-17 September 2009.
3. Scott, G. P., Henshaw, C. G. (2012). "NRL Tests Robotic Fueling of Unmanned Surface Vessels." NRL Press Release 56-12r. 20 March 2012. http://www.nrl.navy.mil/media/news-releases/2012/nrl-test-robotic-fueling-of-unmanned-surface-vessels.
4. Arnold, S. (2010). "NRL Launches Nano-Satellite Experimental Platforms." NRL Press Release 160-10r. 17 December 2010. http://www.nrl.navy.mil/media/news-releases/2010/nrl-launches-nanosatellite-experimental-platforms
5. Tender, L., Gray, S., Groveman, E., Lowy, D., Kauffman, P., Melhado, J., Tyce, R., Flynn, D., Petrecca, R., Dobarro, J. (2008). "The first demonstration of a microbial fuel cell as a viable power supply: Powering a meteorological buoy." Journal of Power Sources. Vol. 179. No. 2. pp 571-575
6. Yi, H., Nevin, K. P., Kim, B-C, Franks, A. E., Klimes, A., Tender, L. M., Lovley, D. R. (2009) "Selection of a variant of *Geobacter sulfurreducens* with enhanced capacity for current production in microbial fuel cells." Journal of Biosensors and Bioelectronics. Vol. 24, pp. 3498-3503.
7. Bond, D. R., Holmes, D. E., Tender, L. M., Lovley, D. R. (2002). "Electrode-Reducing Microorganisms That Harvest Energy from Marine Sediments" *Science*. Vol. 295. No. 5554. pp. 483-485.
8. ONR University Laboratory Initiative (ULI), "Investigation of Microbe-based Proton Exchange Membranes (MPEMs) for Microbial Fuel Cells (MFCs)"
9. He, Z., H. B. Shao, et al. (2007). "Increased power production from a sediment microbial fuel cell with a rotating cathode." Biosensors & Bioelectronics 22(12): 3252-3255.
10. Lowy, D. A. and L. M. Tender (2008). "Harvesting energy from the marine sediment–water interface: III. Kinetic activity of quinone- and antimony-based anode materials." Journal of Power Sources 185(1): 70-75.
11. Reimers, C. E., P. Girguis, et al. (2006). "Microbial fuel cell energy from an ocean cold seep." Geobiology 4(2): 123-136.
12. "99942 Apophis." *Wikipedia*. Wikimedia Foundation, 31 July 2012. Web. 02 Aug. 2012. <http://en.wikipedia.org/wiki/99942_Apophis>.
13. Scott, G. P. (2012). "Navy Researchers Investigate Small-Scale Autonomous Planetary Explorers." NRL Press Release 8-12r. 03 January 2012. http://go.usa.gov/Rqq.

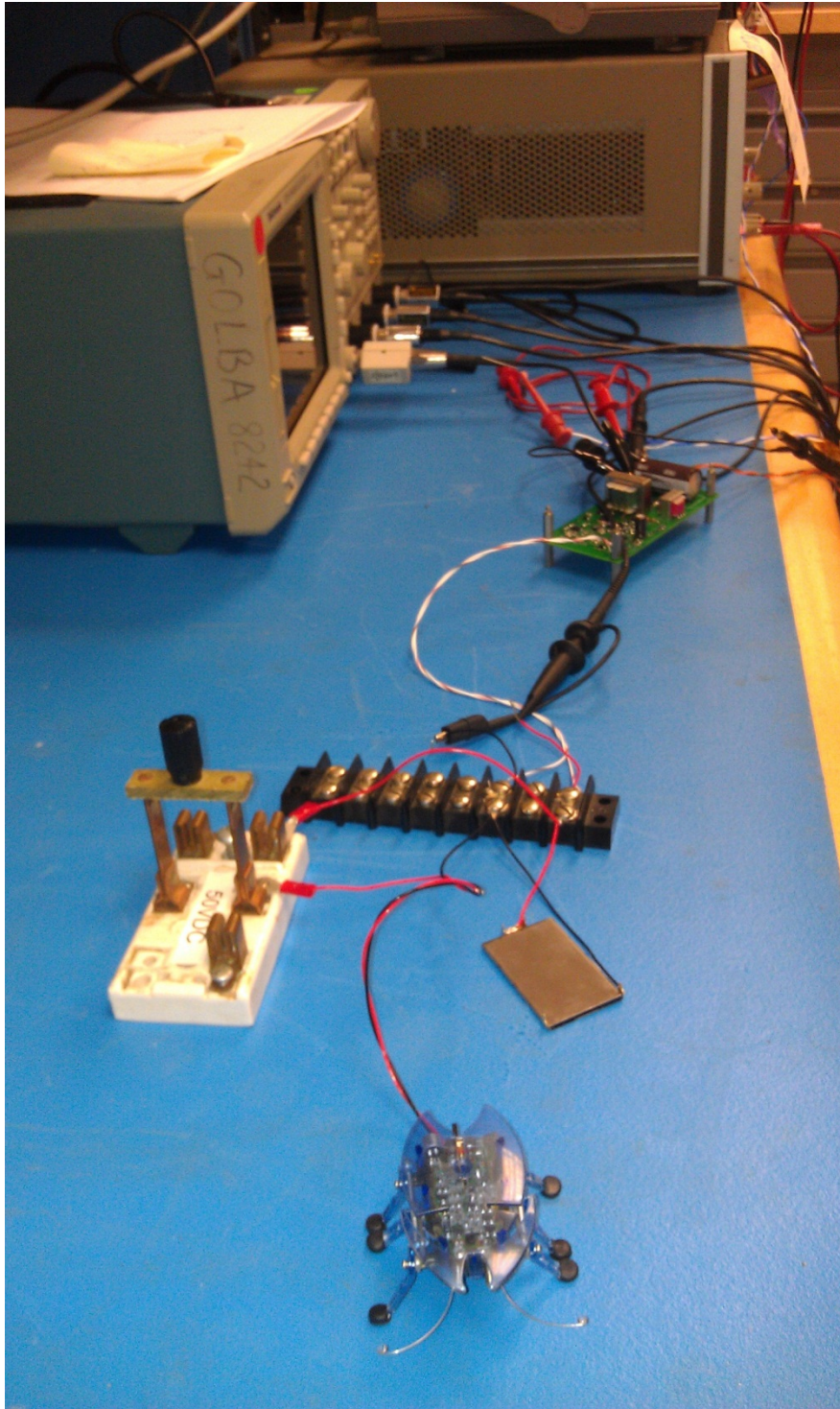# Appendix A – Final Experimental Setup

Figure 31 – The test bench setup for the end-to-end test, including (from bottom to top) the robotic locomotion system, super capacitor, control switch, energy harvesting circuit and oscilloscope.